Electronic Supplementary Material (ESI) for Dalton Transactions.

Supporting Information

Diazo Compounds and Palladium-Aryl Complexes: Trapping the Elusive Carbene Migratory Insertion Organometallic Products

Francisco Villalba and Ana C. Albéniz*
IU CINQUIMA/Química Inorgánica. Universidad de Valladolid. 47071 Valladolid (Spain)]

Table of contents

1. Experimental details

1.1 General considerations

^{1}H, $^{13}C\{^{1}H\}$ ^{31}P and ^{19}F NMR spectra were recorded on Bruker AV-400 or Agilent MR-500 and MR-400 spectrometers equipped with variable-temperature probes at the Laboratorio de Técnicas Instrumentales (LTI) of the UVa. Chemical shifts (in δ units, ppm) were referenced to $SiMe_4$ (^{1}H and ^{13}C) and $CFCl_3$ (^{19}F) and H_3PO_4 (85%, ^{31}P). For the NMR spectra registered in non-deuterated solvents, a coaxial tube containing DMSO-d_6 was used to maintain the lock to the ^{2}H signal. The temperature for the NMR probe was calibrated with a methanol standard (low temperature).[1] Homonuclear (^{1}H-COSY and ^{1}H-ROESY) and heteronuclear (^{1}H-^{13}C HSQC and HMBC) experiments were used to help with the signal assignments. NMR data are given at 298 K unless otherwise noted. Elemental analyses were carried out in a Carlo Erba 1108 microanalyser (at the Vigo University, Spain). Infrared spectra were recorded (in the range 4000-200 cm^{-1}) on a Perkin-Elmer FT-IR Spectrum Frontier with an ATR diamond accessory. All reactions were conducted under a N_2 atmosphere. Solvents were dried using a solvent purification system SPS PS-MD-5 (ether, hexane, THF and CH_2Cl_2) or distilled from appropriate drying agents under nitrogen prior to use and stored over 3 Å or 4 Å molecular sieves (acetonitrile). All commercial reagents and solvents were used as received unless otherwise indicated. The syntheses of the diazo compounds (**3**, **5**) were carried out according to the literature methods.[2] The diazoalkanes were prepared and kept as dichloromethane solutions for no longer than 10 days under a nitrogen atmosphere at -28 ºC in the dark. The concentrations of these solutions were determined by ^{1}H NMR using CF_3CH_2I as internal standard. The palladium complexes $[Pd(Br)(C_6F_5)(dppe)]$,[3] and [PdBr(dppe)Ph],[4] were prepared as reported before.

1.2- Synthesis of Palladium complexes

$[Pd(C_6F_5)(dppe)(NCCH_3)](BF_4)$ (2a). Equimolar amounts of $[Pd(Br)(C_6F_5)(dppe)]$ (152.80 mg, 0.20 mmol) and $AgBF_4$ (39.5 mg, 0.20 mmol) were mixed in dry MeCN (10 mL) and stirred for 15 min at room temperature under nitrogen. The suspension was filtered through Kieselghur and the filtrate was evaporated to dryness. The resulting yellow oil (**2a**) was characterized by NMR (Figures S7-S10). The yellow oil was triturated with diethylether and n-hexane until the formation of a white solid that was filtered, washed with n-hexane and air-dried. Yield: 108.3 mg, (67 %). Upon isolation some reorganization of the aryl groups occur (transmetalation) and this solid is contaminated by small amounts of the reorganization product [Pd(C_6F_5)$_2$(dppe)] (about 3 %).

^{1}H NMR (499.73 MHz, δ, CD_3CN): 7.85 (m, 4H, H^{arom}), 7.75-7.70 (m, 2H, H^{arom}), 7.69-7.52 (m, 10H, H^{arom}), 7.50-7.43 (m, 4H, H^{arom}), 2.92 (m, 2H, CH_2), 2.50 (2H, $C'H_2$). ^{13}C{^{1}H} NMR (125.67 MHz, δ, CD_3CN): 146.5 (m, $^{1}J_{C-F}$ = 227.7 Hz, CF_{ortho}), 138.3 (m, $^{1}J_{C-F}$ = 253 Hz, CF_{para}), 136.3 (m, $^{1}J_{C-F}$ = 254.0 Hz, CF_{para}), 133.2 (d, J_{C-P} = 11.5 Hz, C^{arom}), 133.0 (d, J_{C-P} = 11.8 Hz, C^{arom}), 132.9 (d, J_{C-P} = 3.4 Hz, C^{arom}), 132.6 (d, J_{C-P} = 2.5 Hz, C^{arom}), 129.8 (d, J_{C-P} = 10.5 Hz, C^{arom}), 129.1 (d, J_{C-P} = 11.9 Hz, C^{arom}), 128.0 (d, $^{1}J_{C-P}$ = 45.3 Hz, C^{ipso,arom}), 126.8 (d, $^{1}J_{C-P}$ = 59.9 Hz, C^{ipso,arom}), 29.8 (dd, J_{C-P} = 36.1, 16.6 Hz, CH_2), 22.3 (dd, J_{C-P} = 32.4, 8.1 Hz, CH_2).* ^{19}F NMR (470.17 MHz, δ, CD_3CN): -118.24 (m, 2F, F_{ortho}), -160.39 (t, J = 19.4 Hz, 1F, F_{para}), -163.15 (m, 2F, F_{meta}). ^{31}P{^{1}H} NMR (202.31, MHz, δ, CD_3CN): 62.64 (m, 1P), 52.59 (m, 1P). IR (neat, cm^{-1}): C_6F_5, 1495, 1040, 951, 742, 689; CH_3CN, 2308; BF_4^-, 1046.

*The ^{13}C signal for the C_{ipso} of the C_6F_5 group could not be observed.

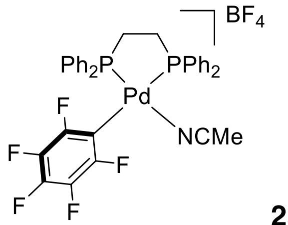

2a

[PdPh(dppe)(NCCH$_3$)](BF$_4$) (2b). [Pd(Br)(dppe)Ph] (12.0 mg, 0.018 mmol) and $AgBF_4$ (3.5 mg, 0.018 mmol) were mixed in dry MeCN (0.6 mL) and stirred for 15 min at room temperature under nitrogen. The suspension was filtered through Kieselghur and the resulting colorless solution was characterized by NMR.

^{1}H NMR (499.73 MHz, δ, CH_3CN,$(CD_3)_2SO$ capillary): 8.04 (m, 4H, H^{arom}), 7.92-7.84 (m, 6H, H^{arom}), 7.81 (m, 2H, H^{arom}), 7.74-7.66 (m, 8H, H^{arom}), 7.27 (m, 2H, H$^{ortho,Pd-Ph}$), 7.08 (m, 2H, H$^{meta\ +\ para,\ Pd-Ph}$), 2.94 (m, 2H, CH_2), 2.62 (m, 2H, CH_2). ^{31}P{^{1}H} NMR (202.31, MHz, δ, CH_3CN,$(CD_3)_2SO$ capillary): 54.51 (d, J = 26.8 Hz, 1P), 41.07 (d, J = 26.8 Hz, 1P).

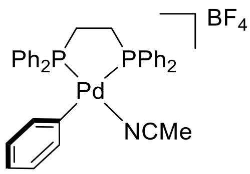

2b

[Pd(dppe)(η^3-Ph-CH-CH-CH-C_6F_5)](BF_4) (4a). [Pd(Br)(C_6F_5)(dppe)] (199.2 mg, 0.265 mmol) and $AgBF_4$ (51.68 mg, 0.265 mmol) were mixed in dry MeCN (5 mL) and stirred for 15 min at room temperature under nitrogen. The resulting suspension was filtered through Kieselghur to remove the AgBr. The addition of a dichloromethane solution of the diazo alkene N_2CH-CH=CHPh (**3**, 12 mL, 0.0248 M) afforded an intense yellow solution, which was stirred at room temperature for 30 min. The solution was evaporated to dryness and the addition of Et_2O (3 mL) led to a yellow solid, which was collected by filtration, washed with cold Et_2O (2 x 5 mL), and air dried. Yield: 0.2 g (86 %)

^{1}H NMR (399.86 MHz, δ, $CDCl_3$): 7.80 (m, 2H, H^{arom}), 7.67 (m, 3H, H^{arom}), 7.47 (m, 5H, H^{arom}), 7.32 (m, 2H, H^{arom}), 7.24 (m, 4H, H^{arom}), 7.11 (t, J = 7.2 Hz, 1H, H_{para}, Ph-allyl), 7.05 (d, J = 7.7 Hz, 2H, H_{ortho} Ph-allyl), 7.00 (m, J = 7.5 Hz, 2H, H_{meta}, Ph-allyl), 6.96 (m, 2H, H^{arom}), 6.83 (m, 2H, H^{arom}), 6.67 (t, J = 13 Hz, 1H, H^2), 5.81 (t, J_{H-H} = J_{H-P} = 13 Hz, 1H, H^1), 5.24 (t, J_{H-H} = J_{H-P} = 13 Hz, 1H, H^3), 2.91 (m, 1H, CH_2), 2.78 (m, 1H, C'H_2), 2.26 (m, 1H, CH_2), 2.0 (m, 1H, C'H_2).† ^{13}C{^{1}H} NMR (100.56 MHz, δ, $CDCl_3$): 143.3 (m, $^1J_{C-F}$ = 250.5 Hz, CF_{ortho}), 137.2 (m, $^1J_{C-F}$ = 252.0 Hz, CF_{para}), 134.5 (d, J_{C-P} = 14.0 Hz, C^{arom}), 133.1 (d, J_{C-P} = 2.4 Hz, C^{arom}), 132.8 (d, J_{C-P} = 13.0 Hz, C^{arom}), 132.1 (d, J_{C-P} = 11.9 Hz, C^{arom}), 131.9 (d, J_{C-P} = 2.5 Hz, C^{arom}), 131.8 (d, J_{C-P} = 2.7 Hz, C^{arom}), 131.1 (d, J_{C-P} = 2.7 Hz, C^{arom}), 130.5 (d, J_{C-P} = 11.3 Hz, C^{arom}), 130.2 (d, J_{C-P} = 11.2 Hz, C^{arom}), 129.6 (d, J_{C-P} = 10.5 Hz, C^{arom}), 129.1 (d, J_{C-P} = 10.6 Hz, C^{arom}), 128.8 ($C_{meta\text{-}Ph\text{-}allyl}$), 128.5 (d, J_{C-P} = 11.3 Hz, C^{arom}), 128.2 ($C_{para\text{-}Ph\text{-}allyl}$), 127.6 (d, $^1J_{C-P}$ = 44.8 Hz, C^{arom}), 126.8 ($C_{ortho\text{-}Ph\text{-}allyl}$), 126.3 (d, $^1J_{C-P}$ = 42.6 Hz, C^{arom}), 125.8 (d, $^1J_{C-P}$ = 45.5 Hz, C^{arom}), 125.2 (d, $^1J_{C-P}$ = 45.3 Hz, C^{arom}), 113.2 (t, J = 6.2 Hz, C^2), 112.3 (m, CF_{ipso}), 96.8 (dd, J_{C-P} = 23.1, 5.5 Hz, C^1), 67.2 (d, J_{C-P} = 30.0 Hz, C^3), 29.0 (dd, J_{C-P} = 33.1, 13.1 Hz, CH_2), 27.1 (dd, J_{C-P} = 32.1, 13.6 Hz, C'H_2).*† ^{19}F NMR (376.19 MHz, δ, $CDCl_3$): -142.11 (m, 2F, F_{ortho}), -157.15 (t, J = 21 Hz, 1F, F_{para}), -161.38 (m, 2F, F_{meta}). ^{31}P{^{1}H} NMR (161.87 MHz, δ, $CDCl_3$): 52.44 (d, J = 48.3 Hz, 1P), 46.70 (d, J = 48.3 Hz, 1P). IR (neat, cm^{-1}): C_6F_5, 1503, 1046, 998, 952, 689; BF_4^- 1040. Anal. Calcd. for $C_{41}H_{32}BF_9P_2Pd$: C, 56.29 %; H, 3.69 %. Found: C, 56.51 %; H, 3.73 %.

† The signal assignment of H^1/C^1 and H^3/C^3 is tentative and could be reversed.

*The ^{13}C signal for the C_{meta} of the C_6F_5 group was not observed.

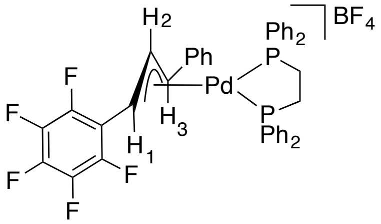

4a

[Pd(dppe)(η^3-Ph-CH-CH-CH-Ph)](BF_4) (4b). [Pd(Br)(C_6H_5)(dppe)] (137.3 mg, 0.207 mmol) and $AgBF_4$ (40.4 mg, 0.207 mmol) were mixed in dry MeCN (3 mL) and stirred for 15 min at room temperature under nitrogen. The suspension was filtered through Kieselghur to remove the AgBr. The addition of a dichloromethane solution of the diazo compound N_2CH-CH=CHPh (**3**, 2.3 mL, 0.09 M) afforded an intense yellow solution, which was stirred at room temperature for 30 min. The solution was evaporated to dryness and the addition of Et_2O (5 mL) afforded complex **4b** as a yellow solid, which was collected by filtration, washed with cold Et_2O (2 x 5 mL), and air dried. Yield: 0.130 g (80 %).

^1H NMR (399.86 MHz, δ, $CDCl_3$): 7.53 (m, 6H, H^{arom}), 7.45 (m, 4H, H^{arom}), 7.35 (t, J = 7.2 Hz, 2H, H^1), 7.16 (t, J= 7.3 Hz, 4H, H^2), 7.02 (m, 6H, H^{arom}), 6.93 (m, 4H, H^{arom}), 6.76 (m, 4H, H^3), 6.59 (t, J = 12.9 Hz, 1H, H^6), 5.46 (m, 2H, H^5), 2.51-2.33 (m, 4H, CH_2). $^{13}C\{^1H\}$ NMR (100.56 MHz, δ, $CDCl_3$): 136.3 (t, J_{C-P} = 4.6 Hz, C^4), 133.3 (t, J_{C-P} = 6.4 Hz, C^{arom}), 131.9 (C^{arom}), 131.6 (t, J_{C-P} = 5.7, C^3), 131.1 (C^1), 129.7 (t, J_{C-P} = 5.5 Hz, C^{arom}), 129.3 (t, J_{C-P} = 5.2 Hz, C^2), 128.7 (t, J_{C-P} = 1.9 Hz, C^{arom}), 128.0 (m, $C^{ipso-arom}$), 127.4 (t, J_{C-P} = 2.6 Hz, C^{arom}), 126.8 (t, J_{C-P} = 3.1 Hz, C^{arom}), 126.6 (m, $C^{ipso-arom}$), 111.6 (t, J_{C-P} = 7.3 Hz, C^6), 90.1 (t, J_{C-P} = 15.8 Hz, C^5), 28.0 (t, J_{C-P} = 23.0 Hz, CH_2). $^{31}P\{^1H\}$ NMR (161.87 MHz, δ, $CDCl_3$): 46.38 (s, 2P). IR (neat, cm^{-1}): BF_4, 1044 br. Anal. Calcd. for $C_{41}H_{37}BF_4P_2Pd$: C, 62.74 %; H, 4.75 %. Found: C, 62.79 %; H, 4.79 %.

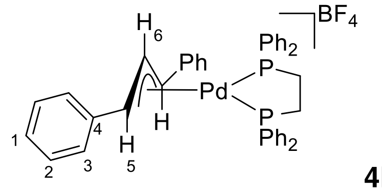

4b

[Pd(dppe)(η^3-Ph-CH-Pf)](BF_4) (6). Equimolar amounts of [Pd(Br)(C_6F_5)(dppe)] (113.23 mg, 0.150 mmol) and $AgBF_4$ (29.32 mg, 0.150 mmol) were mixed in dry MeCN (5 mL) and stirred for 15 min at room temperature under nitrogen. The suspension was filtered through Kieselghur to remove the AgBr. Addition of a dichloromethane solution of the diazo compound N_2CHPh (**5**, 1 mL, 0.146 M) afforded an intense yellow solution, which was stirred at room temperature for 30 min. Then, the solution was evaporated to dryness to give a yellow residue, which was triturated with n-hexane (3 mL) affording a yellow solid. The yellow solid was collected by filtration, washed with n-hexane (2 x 5 mL), and air dried. Yield: 63.31 mg (50 %).

^{1}H NMR (399.86 MHz, δ, $CDCl_3$, 298 K): 7.82 (m, 2H, H^{arom}), 7.6-7.68 (m, 3H, H^{arom}), 7.48-7.57 (m, 6H, H^{arom}), 7.35-7.45 (m, 6H, H^{arom}), 7.16 (td, J = 7.9, 2.5 Hz, 2H, H^{arom}), 6.98 (m, br, 1H, H^6), 6.80 (m, 4H, H^{arom}), 6.75 (m, br, 1H, H^2), 4.54 (d, $^3J_{H\text{-}P}$ = 12.3 Hz, 1H, H^{α}), 2.94 (m, 2H, CH_2, $C'H_2$), 2.28 (m, 1H, CH_2), 1.92 (m, 1H, $C'H_2$). $^{13}C\{^1H\}$ NMR (100.56 MHz, δ, $CDCl_3$, 298 K): 143.6 (m, $^1J_{C\text{-}F}$ = 248.8 Hz, CF_{ortho}), 137.2 (m, $^1J_{C\text{-}F}$ = 251.3 Hz, CF_{para}), 134.7 (d, $J_{C\text{-}P}$ = 13.7 Hz, C^{arom}), 133.3 (C^{arom}), 132.8 (d, $J_{C\text{-}P}$ = 13.5 Hz, C^{arom}), 132.4 (C^{arom}), 131.8 (d, $J_{C\text{-}P}$ = 12.4 Hz, C^{arom}), 130.9 (d, $J_{C\text{-}P}$ = 2.2 Hz, C^{arom}), 130.3 (d, $J_{C\text{-}P}$ = 10.9 Hz, C^{arom}), 130.2 (d, $J_{C\text{-}P}$ = 9.7 Hz, C^{arom}), 129.7 (d, $J_{C\text{-}P}$ = 10.3 Hz, C^{arom}), 129.6 (d, $J_{C\text{-}P}$ = 9.9 Hz, C^{arom}), 129.2 (t, $J_{C\text{-}P}$ = 4.1 Hz, C^{arom}), 128.8 (d, $J_{C\text{-}P}$ = 10.9 Hz, C^{arom}), 128.4 (d, $^1J_{C\text{-}P}$ = 49.9 Hz, C^{arom}), 127.0 (d, $^1J_{C\text{-}P}$ = 48.9 Hz, C^{arom}), 126.1 (d, $^1J_{C\text{-}P}$ = 46.1 Hz, C^{arom}), 125.2 (d, $^1J_{C\text{-}P}$ = 42.0 Hz, C^{arom}), 125.4 (br, C^6), 120.7 (dd, $J_{C\text{-}P}$ = 8.5, 3.8 Hz, C^1), 112.3 (t, $^2J_{C\text{-}F}$ = 15.5 Hz, CF_{ipso}), 100.6 (br, C^2), 49.6 (dd, J = 48.8, 11.0 Hz, C^{α}), 28.3 (dd, $J_{C\text{-}P}$ = 34.5, 15.2 Hz, CH_2), 24.2 (dd, $J_{C\text{-}P}$ = 31.2, 10.6 Hz, $C'H_2$).* ^{19}F NMR (376.19 MHz, δ, $CDCl_3$, 298 K): -136.41 (m, 2F, F_{ortho}), -157.44 (t, J = 21.1 Hz, 1F, F_{para}), -160.87 (m, 2F, F_{meta}). $^{31}P\{^1H\}$ NMR (161.87 MHz, δ, $CDCl_3$, 298 K): 57.76 (dm, J = 49.8 Hz, 1P), 46.91 (dd, J = 49.8, 3.0 Hz, 1P). IR (neat, cm^{-1}): C_6F_5, 1435, 1050, 996, 964, 690; BF_4^-, 1054. Anal. Calcd. for $C_{39}H_{30}BF_9P_2Pd$: C, 55.19 %; H, 3.56 %. Found: C, 55.51 %; H, 3.46 %

* ^{13}C signals for the C_{para} and C_{meta} of the benzylic fragment could not be located.

^{1}H NMR (499.73 MHz, δ, $CDCl_3$, 226 K): 7.88 (m, 2H, H^{arom}), 7.73-7.30 (m, 15H, H^{arom}, H^3, H^5), 7.17 (t, J = 7.6 Hz, 2H, H^{arom}), 6.98 (s, 1H, H^6), 6.74 (m, 4H, H^{arom}), 6.58 (s, 1H, H^2), 4.47 (d, $^3J_{H\text{-}P}$ = 12.3 Hz, 1H, H^{α}), 2.94 (m, 2H, CH_2, $C'H_2$), 2.16 (m, 1H, CH_2), 1.86 (m, 1H, $C'H_2$).* ^{19}F NMR (470.17 MHz, δ, $CDCl_3$, 226 K): -156.96 (t, J =

21.9 Hz, 1F, F_{para}), -160.11 (m, 2F, F_{meta}).† $^{31}P\{^{1}H\}$ NMR (202.31 MHz, δ, $CDCl_3$, 226 K): 59.15 (d, J = 48.1 Hz, 1P), 47.28 (d, J = 48.1 Hz, 1P).

† Restricted rotation about the C-C_6F_5 bond leads to coalescence of the F_{ortho} signals at 226 K and they could not be observed.

The stereochemistry of the complex was unequivocally determined by the observation of a positive NOE effect observed between H^{α} and H^{2} in a ^{1}H 2D-ROESY experiment at 226 K.

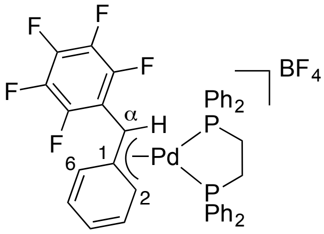

6

1.3 Attempts at detection of intermediate complexes before the migratory insertion

$[Pd(C_6F_5)(NCMe)(dppe)]BF_4$ (**2a**) (0.0175 mmol) and 0.6 mL of dry CD_2Cl_2 were added into an NMR tube under a nitrogen atmosphere, and placed in cooled bath at -105 ˚C. Then, 1.5 equivalents of a precooled diazo compound (-50 ˚C) were added and the tube was closed. The resulting mixture was frozen during the setup of the NMR-experiment. Finally, the NMR tube was introduced into another cool bath at -90 ˚C for 5 minutes to allow the equilibration of the temperature. After this time, the sample was shaken vigorously inside the cool bath, wiped externally and introduced in the NMR probe already set at the measurement temperature (-90 ˚C). The reaction was monitored by ^{19}F NMR, at -90 ˚C first and then at higher temperature (10 degree intervals).

Figure S1 shows the mixture of palladium complexes formed when **2a** was dissolved in CD_2Cl_2 at -90 ˚C. A small amount of Et_2O in the sample along with a slow ligand exchange at that temperature leads to the coexistence of **2a** and $[Pd(C_6F_5)(dppe)(OEt_2)]BF_4$. Analogous species have been reported before.[5] The latter is transformed in **2a** upon addition of MeCN. The reorganization product $[Pd(C_6F_5)_2(dppe)]$ (3 %) was also present, which was formed during the isolation of complex **2a** (see above).

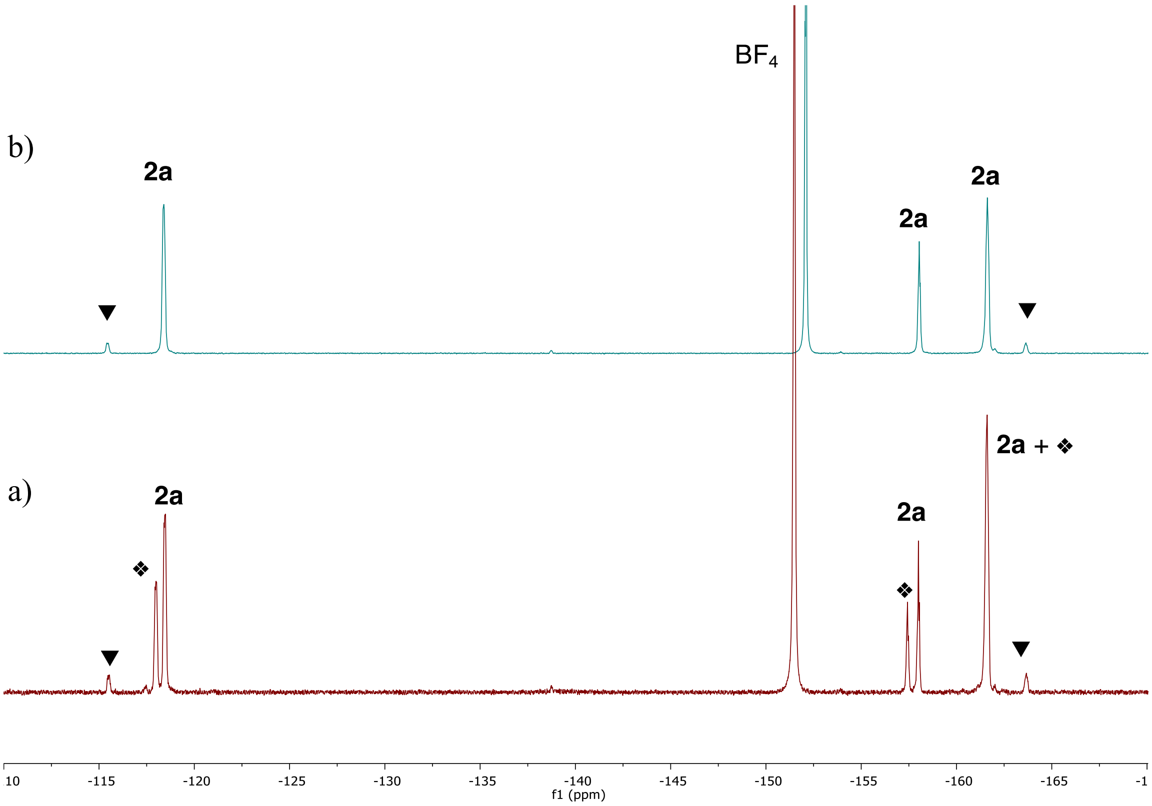

Figure S1. ^{19}F NMR (376.46 MHz, δ, CD_2Cl_2) at -90 ˚C of: a) a mixture of complexes **2a**, $[Pd(C_6F_5)(dppe)(OEt_2)]BF_4$ (◆) and $[Pd(C_6F_5)_2(dppe)]$ (▼) formed when a sample of **2a** was dissolved in dichloromethane at low temperature ; b) the mixture shown in (a) upon addition of MeCN (10 equivalents).

Figure S2 shows the variable temperature follow up of the reaction of **2a** with N_2CHPh (**5**). Scheme S1 depicts the products found in this reaction at -90 ˚C.

The analogous reaction with $N_2CH\text{-}CH{=}CHPh$ (**3**) is shown in Scheme S2 and the variable temperature monitorization in Figure S3.

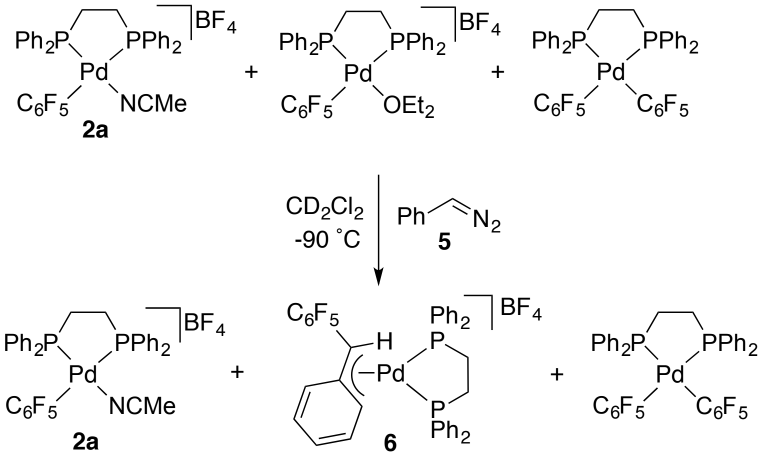

Scheme S1. Reaction of the solvento complexes [Pd(C_6F_5)(dppe)S]BF_4. (S = MeCN, OEt_2) with N_2CHPh (**5**, 1.5 equivalents) at -90 ˚C in CD_2Cl_2 (see Figure S2, a and b).

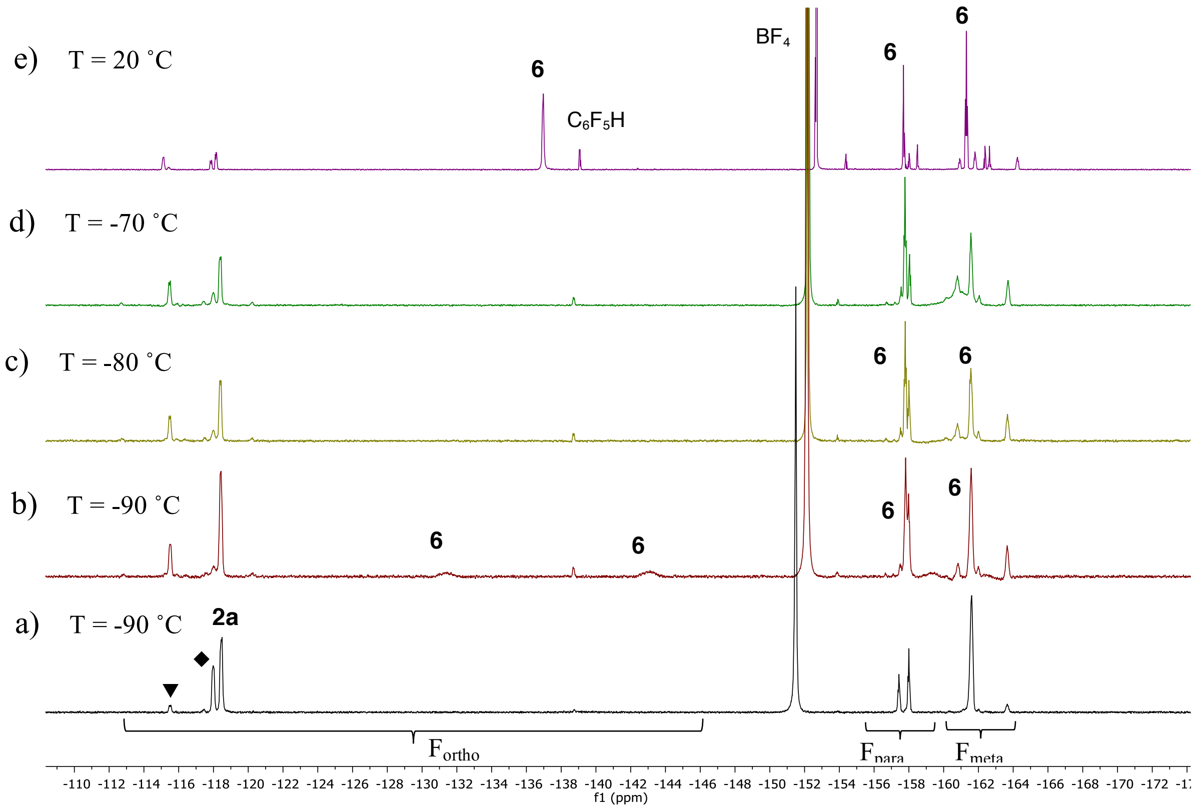

Figure S2. ^{19}F NMR (376.46 MHz, δ, CD_2Cl_2) of: a) a mixture of complexes **2a**, [Pd(C_6F_5)(dppe)(OEt_2)]BF_4 (◆) and [Pd(C_6F_5)$_2$(dppe)] (▼) formed when a sample of **2a** was dissolved in dichloromethane at low temperature ; b) the mixture shown in (a) upon addition of N_2CHPh (**5**, 1.5 equivalents); c) the mixture shown in (b) at -80 ˚C; d) the mixture shown in (c) at -70 ˚C; e) the mixture shown in (d) at room temperature. Slow rotation of the C_6F_5 group is observed at low temperature for complex **6**: broad F_{ortho} signals at -90 ˚C (b) and the disappearance of the F_{ortho} resonances due to coalescence in the range -80 to -70 ˚C (c and d).

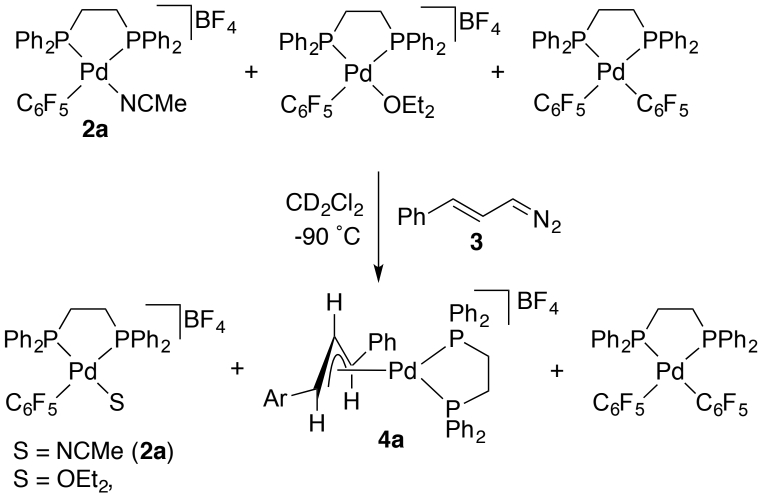

Scheme S2. Reaction of the solvento complexes $[Pd(C_6F_5)(dppe)S]BF_4$. (S = MeCN, OEt_2) with $N_2CH\text{-}CH\text{=}CHPh$ (**3**, 1.5 equivalents) at -90 ˚C in CD_2Cl_2 (see Figure S3, a and b)

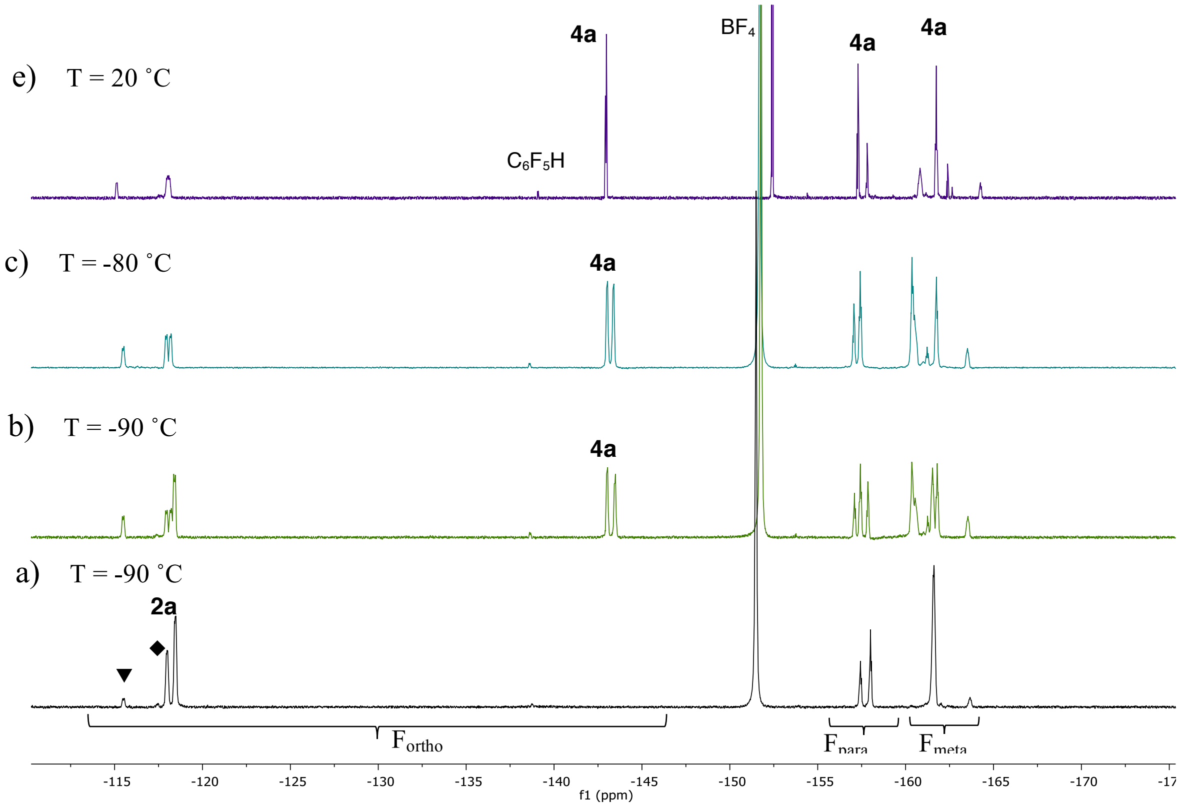

Figure S3. ^{19}F NMR (376.46 MHZ, δ, CD_2Cl_2) of: a) a mixture of complexes **2a**, $[Pd(C_6F_5)(dppe)(OEt_2)]BF_4$ (◆) and $[Pd(C_6F_5)_2(dppe)]$ (▼) formed when a sample of **2a** was dissolved in dichloromethane at low temperature; b) the mixture shown in (a) upon addition of $N_2CH\text{-}CH\text{=}CHPh$ (**3**, 1.5 equivalents); c) the mixture shown in (b) at -80 ˚C; d) the mixture shown in (c) at room temperature. Slow rotation of the C_6F_5 group is observed at low temperature for complex **4a** shown by the inequivalent of F_{ortho} signals (b and c) that become equivalent due to fast rotation at room temperature (d).

2. Data for X-Ray molecular structure determinations

Crystals suitable for X-ray analyses for were obtained by slow diffusion of n-hexane layered onto a solution of the complex in CH_2Cl_2 at -28 ˚C. In each case, the crystal was attached to the tip of a glass fiber and transferred to an Agilent Supernova diffractometer with an Atlas CCD area detector. Data collection was performed with Mo Kα radiation (0.71073 Å) at 298 K. Data integration and empirical absorption correction was carried out using the CrysAlisPro program package.[6] The structures were solved by direct methods and refined by full-matrix least squares against F^2 with SHELX,[7] in OLEX2.[8] The non-hydrogen atoms were refined anisotropically and hydrogen atoms were constrained to ideal geometries and refined with fixed isotropic displacement parameters. Refinement proceeded smoothly to give the residuals shown in Table S3.

The crystal structures have been deposited in the CCDC database: CCDC-2184725 (complex **4a**); CCDC-2184716 (complex **6**).

Table S1. Crystal data and structure refinement parameters for complexes **4a** and **6**.

Compound number	**4a**	**6**
Empirical formula	$C_{41}H_{32}BF_9P_2Pd$	$C_{39}H_{30}BF_9P_2Pd$
Formula weight	874.81	848.78
Temperature/K	298	298.15
Crystal system	monoclinic	triclinic
Space group	$P2_1/n$	P-1
a/Å	10.1431(4)	8.5211(4)
b/Å	22.7544(7)	10.1127(4)
c/Å	16.9793(5)	21.1960(7)
α/°	90	91.301(3)
β/°	104.335(4)	95.754(3)
γ/°	90	93.117(4)
Volume/Å^3	3796.8(2)	1813.87(13)
Z	4	2
ρ_{calc}g/cm^3	1.530	1.554
μ/mm^{-1}	0.647	0.675
F(000)	1760.0	852.0
Crystal size/mm^3	0.269 × 0.17 × 0.057	0.253 × 0.161 × 0.049
Radiation	MoKα (λ = 0.71073)	MoKα (λ = 0.71073)

2Θ range for data collection/°	6.662 to 59.076	6.91 to 59.392
Index ranges	$-13 \leq h \leq 13$, $-31 \leq k \leq 23$, $-23 \leq l \leq 17$	$-10 \leq h \leq 10$, $-12 \leq k \leq 13$, $-29 \leq l \leq 29$
Reflections collected	20113	13812
Independent reflections	8931 [R_{int} = 0.0370, R_{sigma} = 0.0641]	8440 [R_{int} = 0.0336, R_{sigma} = 0.0759]
Data/restraints/parameters	8931/0/487	8440/0/469
Goodness-of-fit on F^2	1.033	1.069
Final R indexes [I>=2σ (I)]	R_1 = 0.0544, wR_2 = 0.1122	R_1 = 0.0552, wR_2 = 0.0922
Final R indexes [all data]	R_1 = 0.0961, wR_2 = 0.1320	R_1 = 0.0891, wR_2 = 0.1114
Largest diff. peak/hole / e Å^{-3}	1.23/-0.52	0.43/-0.46

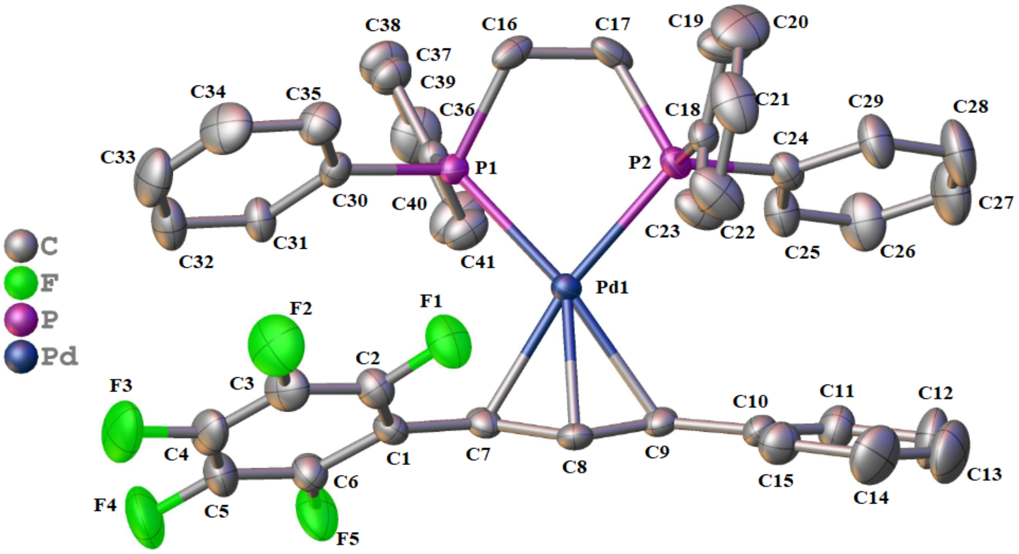

Figure S4. X-ray molecular structure of **4a** (ORTEP 40% probability ellipsoids). Hydrogen atoms and the BF_4^- anion are omitted for clarity.

Table S2. Selected bond lengths (Å) and angles (°) for complex **4a** (for numbering scheme see Figure S4).

Pd(1)-P(1)	2.2881(10)	P(1)-Pd(1)-P(2)	85.17(4)
Pd(1)-P(2)	2.2914(10)	C(7)-Pd(1)-C(9)	66.27(15)
Pd(1)-C(7)	2.179(4)	C(9)-C(8)-C(7)	119.4(4)
Pd(1)-C(8)	2.177(4)		
Pd(1)-C(9)	2.253(4)		
C(7)-C(8)	1.416(5)		
C(8)-C(9)	1.392(6)		

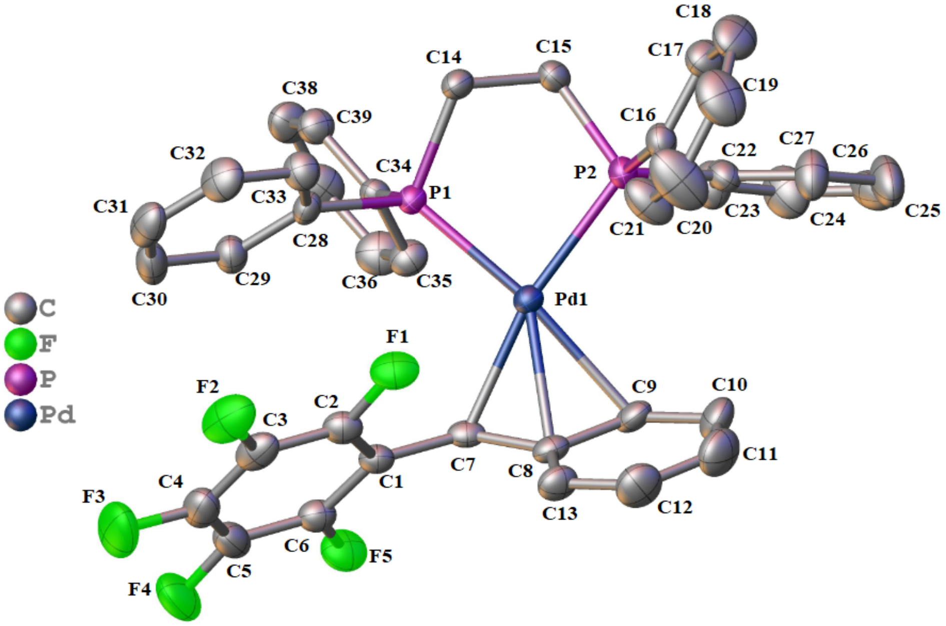

Figure S5. X-ray molecular structure of **6** (ORTEP 40% probability ellipsoids). Hydrogen atoms and the BF_4^- anion are omitted for clarity.

Table S3. Selected bond lengths [Å] and angles [º] for complex **6** (for numbering scheme see Figure S5).

Pd(1)-P(1)	2.2609(11)	C(8)-C(9)	1.417(5)
Pd(1)-P(2)	2.3018(10)	C(8)-C(13)	1.418(5)
Pd(1)-C(7)	2.155(4)	C(13)-C(12)	1.347(6)
Pd(1)-C(8)	2.275(4)	C(12)-C(11)	1.393(7)
Pd(1)-C(9)	2.284(4)	C(11)-C(10)	1.350(7)
C(7)-C8)	1.447(6)	C(10)-C(9)	1.405(6)
P(1)-Pd(1)-P(2)	86.25(4)	C(7)-Pd(1)-C(9)	66.80(15)
C(7)-C(8)-C(9)	117.3(3)		

3. Computational Details.

3.1 Computational Methods.

All calculations were performed using the DFT approach with the meta-hybrid GGA M06 functional,[9,10] using Gaussian09 as program package.[11] The selected basis set was 6-31+G(d) for C, N, F and H[12,13], and LANL2TZ(f) for Pd[14,15] (Basis set I). Solvation was introduced in all the optimizations, frequency calculations and potential energy refinement through the SMD model, where we applied the experimental solvent, acetonitrile ($\varepsilon = 37.5$, at 25 ˚C). All geometry optimizations were carried out in solution with no symmetry restrictions. Free energy corrections were calculated at 298.15 K and 10^5 Pa pressure, including zero-point energy corrections (ZPE), and the energies were converted to 1M standard state in solution (adding/substracting 1.89 kcal/mol for non-unimolecular processes). Vibrational frequency calculations were performed to establish the stationary points were minima (without imaginary frequencies) or transition states (with one imaginary frequency). Connectivity of the transition state structures were confirmed by relaxing the transition state geometry towards both the reactant and the product. Final potential energies were refined by performing additional single-point energy calculations (also in solution), Pd was still described with LANL2TZ(f) basis set, and the remaining atoms were treated with 6- 311++G(d,p) basis set (Basis set II). All reported energies in the manuscript correspond to Gibbs energies in solution, obtained from potential energies (including solvation) with basis set II plus Gibbs energy corrections with basis set I and are given in kcal mol^{-1}.

3.2 Free energy profile.

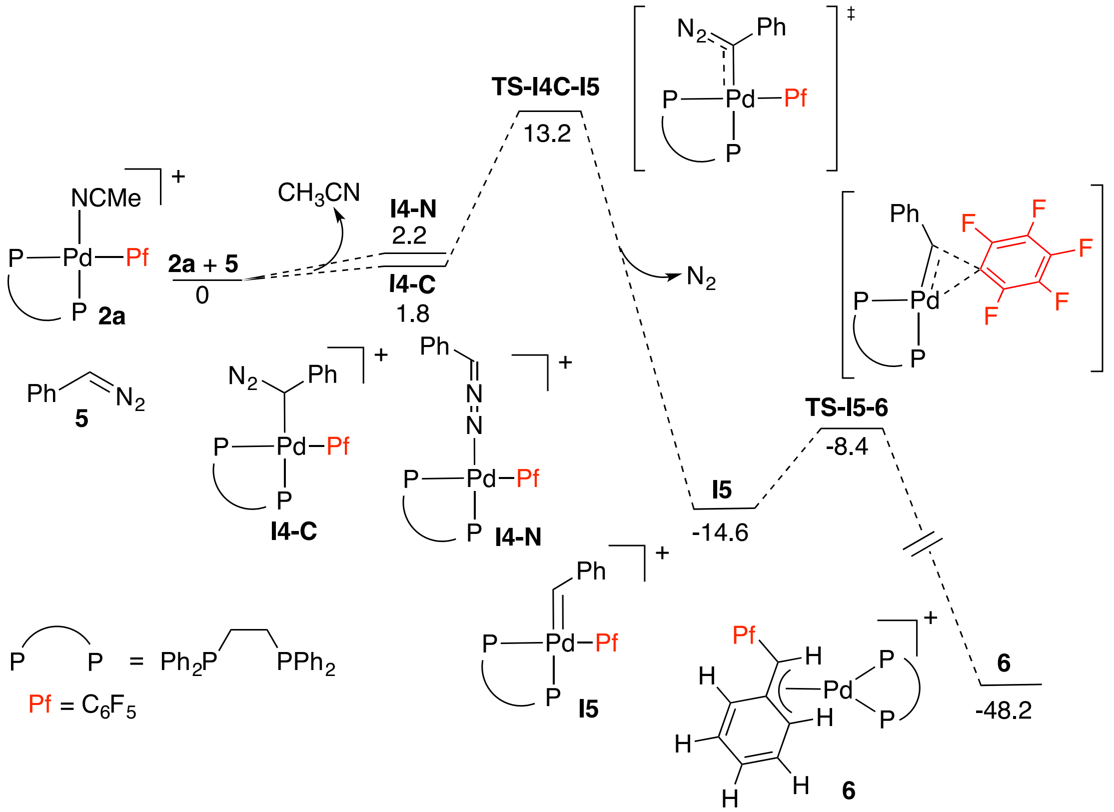

Figure S6. Free-energy profile for the reaction of complex **2a** and the diazo compound **5** to give the migratory insertion complex **6**. Energies in kcal mol^{-1}.

3.3 Calculated Potential Energies (atomic units).

SCF energy at high basis set level (Basis set II) and free energy correction at low basis set level (Basis set I). Then sum of both energies provides the final free energy of each compound used in the manuscript. Cartesian Coordinates (Å) can be found in a separate .xyz formatted document.

NCMe
SCF Energy = -132.7043236000
Thermal Correction to Gibbs Free Energy = 0.021396

N$_2$
SCF Energy = -109.4851699000
Thermal Correction to Gibbs Free Energy = -0.012817

3
SCF Energy = -456.9843711000
Thermal Correction to Gibbs Free Energy = 0.113084

2a
SCF Energy = -2674.4945438000
Thermal Correction to Gibbs Free Energy = 0.447408

I1-N
SCF Energy = -2998.7751202000
Thermal Correction to Gibbs Free Energy = 0.545220

I1-C
SCF Energy = -2998.7746861000
Thermal Correction to Gibbs Free Energy = 0.544117

I1-alkene
SCF Energy = -2998.7833619000
Thermal Correction to Gibbs Free Energy = 0.545854

I2
SCF Energy = -2889.3048001000
Thermal Correction to Gibbs Free Energy = 0.535992

I3
SCF Energy = -2889.3562344000
Thermal Correction to Gibbs Free Energy = 0.542396

4a
SCF Energy = -2889.3843871000
Thermal Correction to Gibbs Free Energy = 0.541635

TS-I1C-I2
SCF Energy = -2998.7552974000
Thermal Correction to Gibbs Free Energy = 0.542265

TS-I2-I3
SCF Energy = -2889.2956795000
Thermal Correction to Gibbs Free Energy = 0.536691

5
SCF Energy = -379.622972600
Thermal Correction to Gibbs Free Energy = 0.081846

I4-N
SCF Energy = -2921.412790000
Thermal Correction to Gibbs Free Energy = 0.511007

I4-C
SCF Energy = -2921.415587100
Thermal Correction to Gibbs Free Energy = 0.513123

I5
SCF Energy = -2811.937115300
Thermal Correction to Gibbs Free Energy = 0.503564

6
SCF Energy = -2811.995810500
Thermal Correction to Gibbs Free Energy = 0.5086130

TS-I4C-I5
SCF Energy = -2921.396428300
Thermal Correction to Gibbs Free Energy = 0.512164

TS-I5-6
SCF Energy = -2811.930409200
Thermal Correction to Gibbs Free Energy = 0.506717

4. Selected spectra

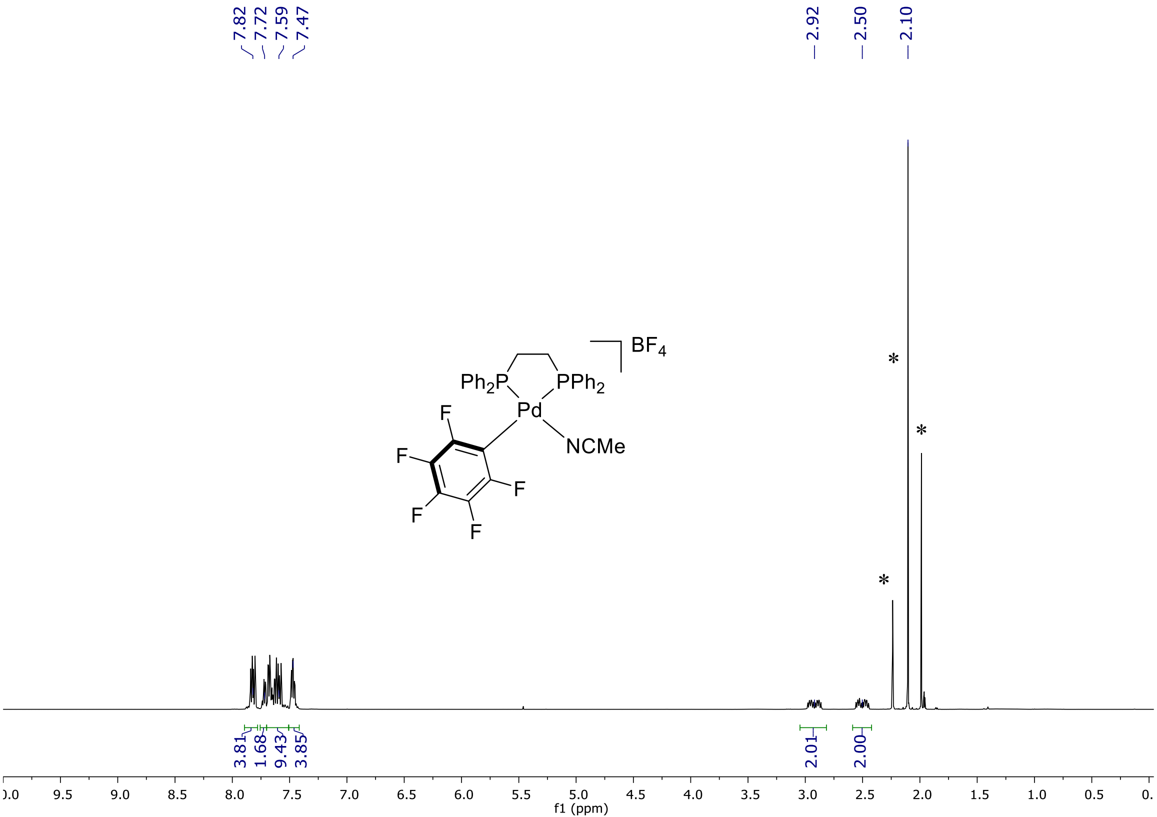

Figure S7. ^{1}H NMR (499.73 MHz, CD_3CN) of [Pd(C_6F_5)(dppe)($NCCH_3$)](BF_4) (**2a**) at 298 K. * Signals corresponding to the solvent (H_2O, acetonitrile and acetone).

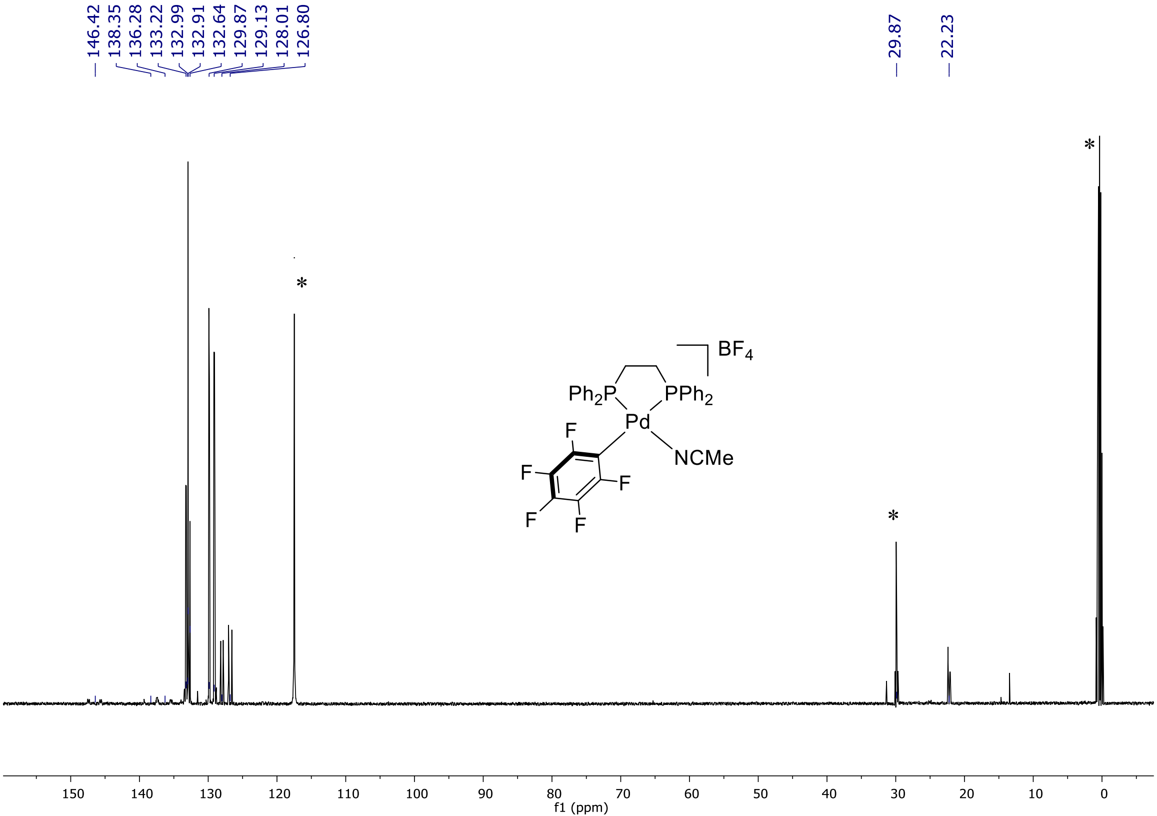

Figure S8. ^{13}C{^{1}H} NMR (125.67 MHz, CD_3CN) of [Pd(C_6F_5)(dppe)($NCCH_3$)](BF_4) (**2a**) at 298 K. * Signals corresponding to the solvent (acetonitrile and acetone).

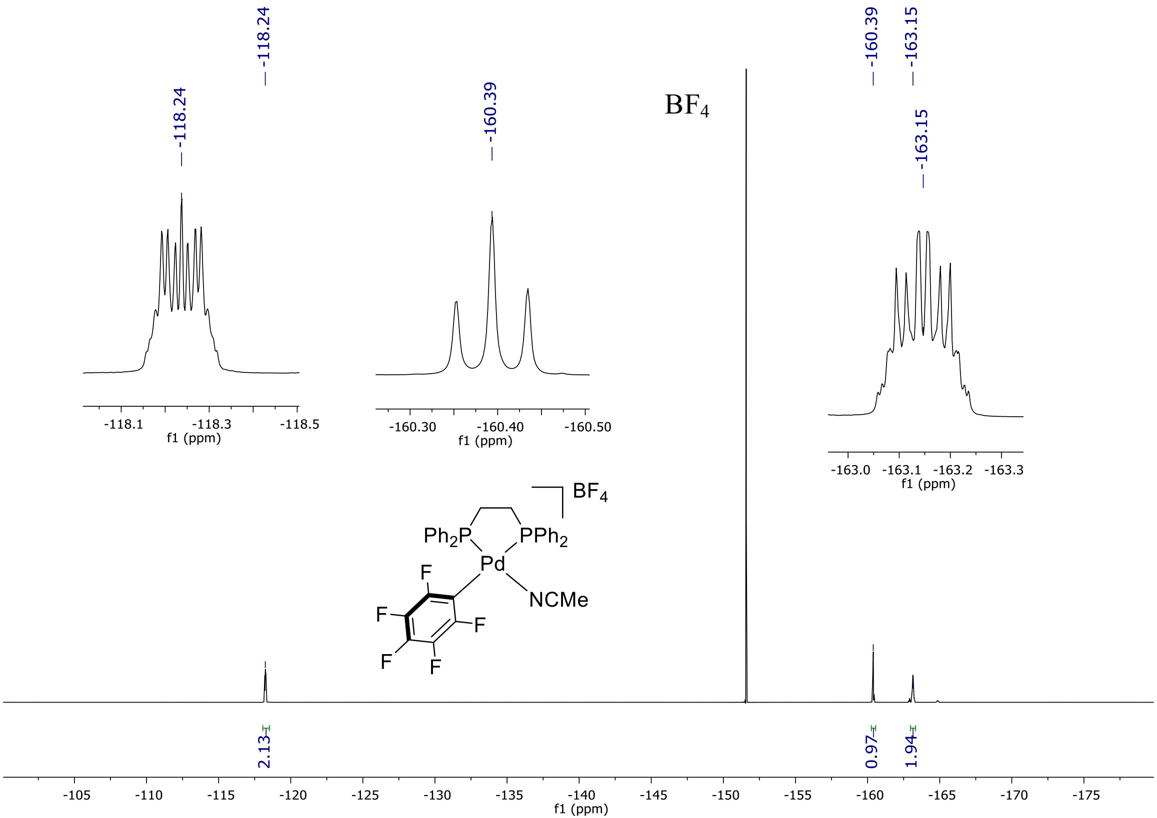

Figure S9. ^{19}F NMR (470.17 MHz, CD_3CN) of $[Pd(C_6F_5)(dppe)(NCCH_3)](BF_4)$ (**2a**) at 298 K.

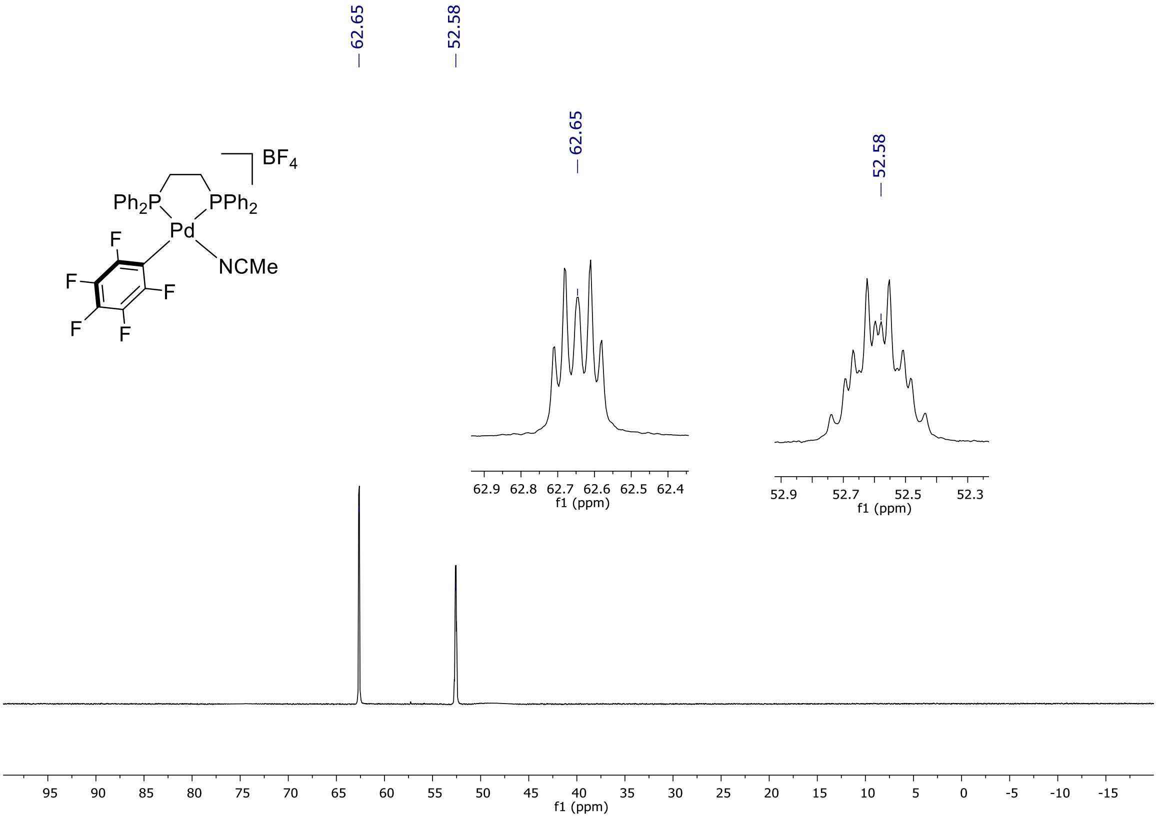

Figure S10. ^{31}P NMR (202.31 MHz, CD_3CN) of $[Pd(C_6F_5)(dppe)(NCCH_3)](BF_4)$ (**2a**) at 298 K.

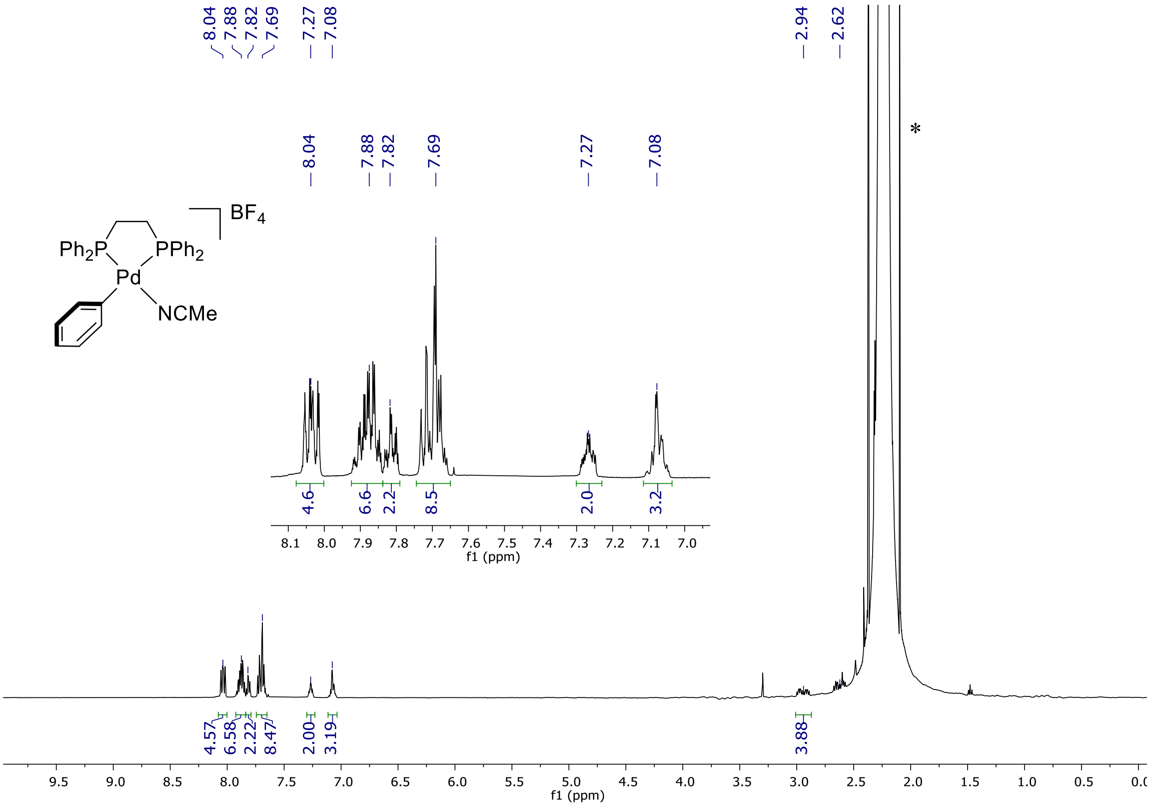

Figure S11. ^{1}H NMR (499.73 MHz, CH_3CN, $(CD_3)_2SO$ capillary) of [Pd(dppe)(NCMe)Ph](BF_4) (**2b**) at 298 K. * Signals corresponding to the solvent (CH_3CN).

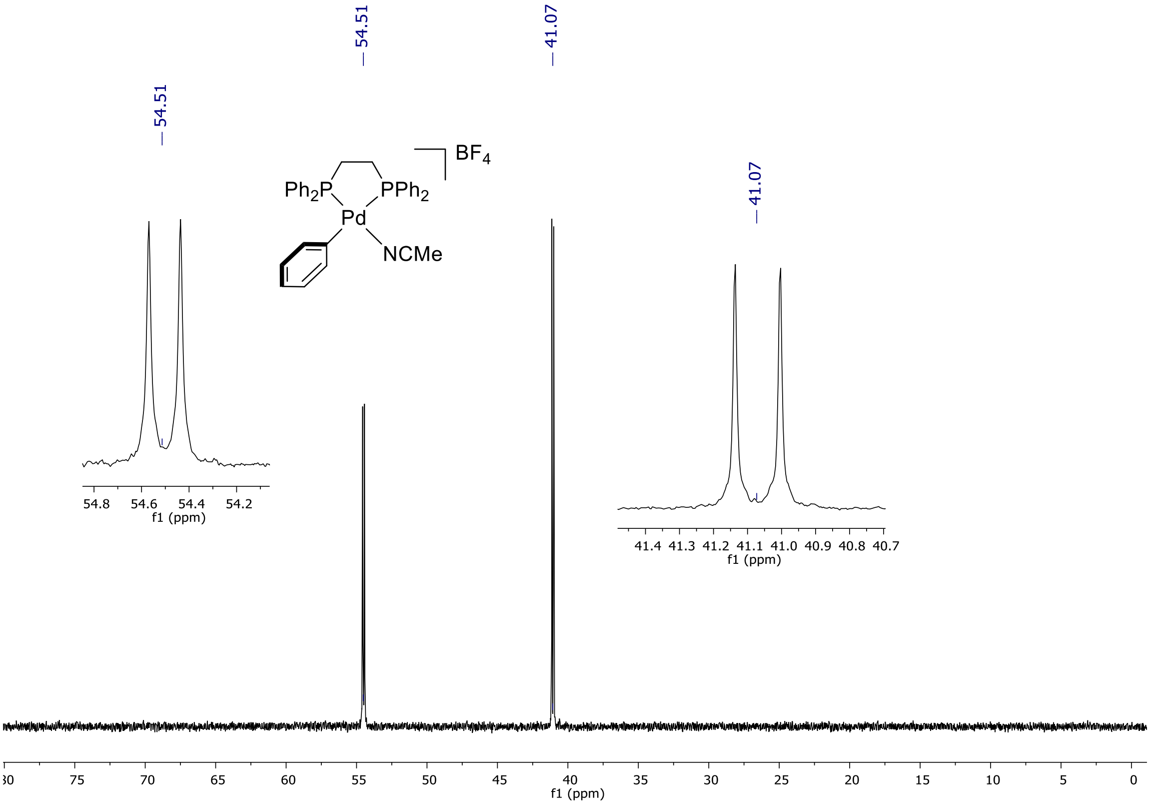

Figure S12. ^{31}P NMR (202.31 MHz, CH_3CN, $(CD_3)_2SO$ capillary) of [Pd(dppe)(NCMe)Ph](BF_4) (**2b**) at 298 K.

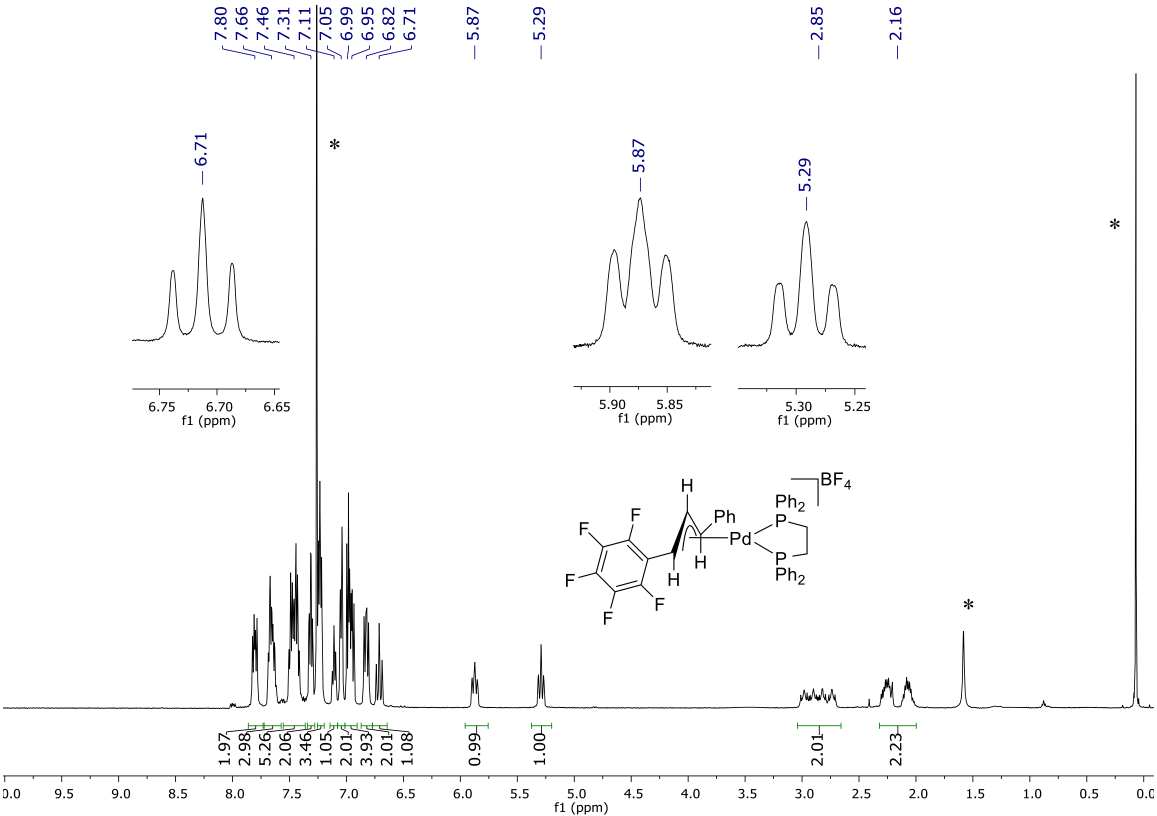

Figure S13. ^{1}H NMR (399.86 MHz, CDCl$_3$) of [Pd(dppe)(η^3-Ph-CH-CH-CH-Pf)](BF$_4$) (**4a**) at 298 K. * Signals corresponding to the solvent (H$_2$O, chloroform and silicone grease).

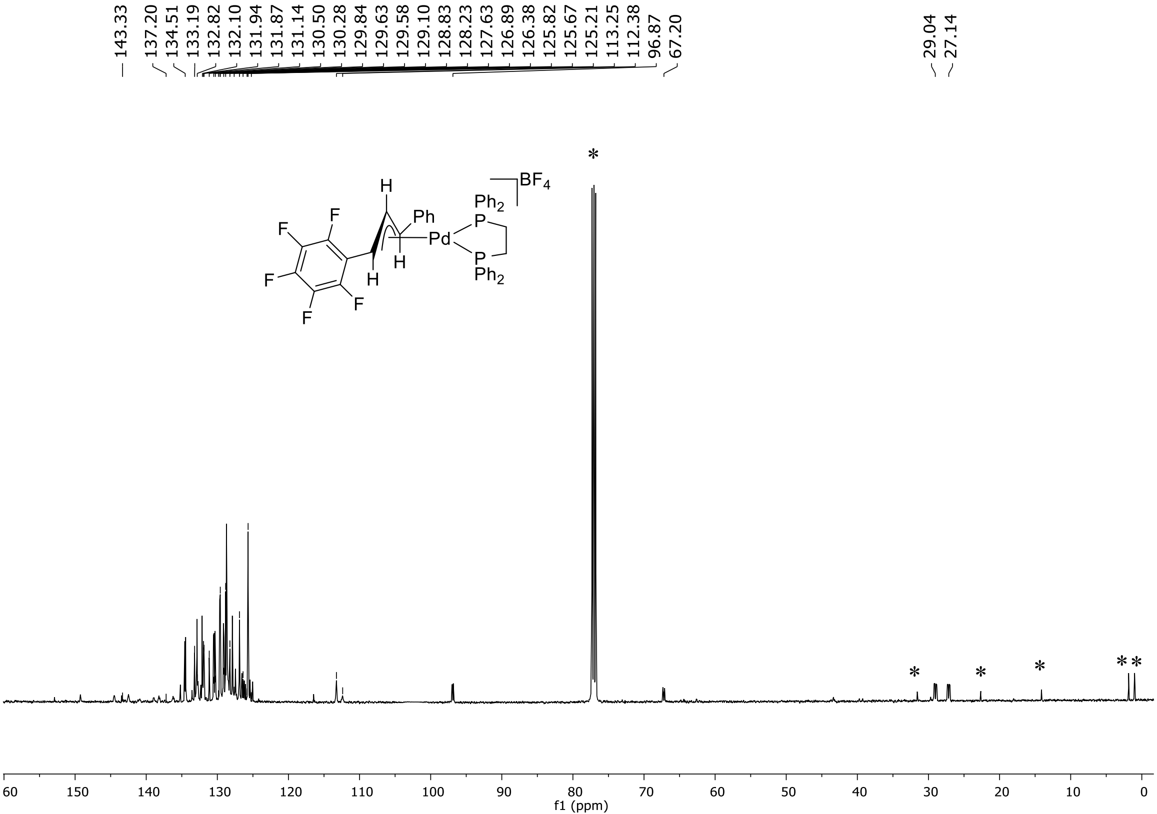

Figure S14. ^{13}C{^{1}H} NMR (100.56 MHz, CDCl$_3$) of [Pd(dppe)(η^3-Ph-CH-CH-CH-Pf)](BF$_4$) (**4a**) at 298 K. * Signals corresponding to the solvent (chloroform, traces of hexanes and silicone grease).

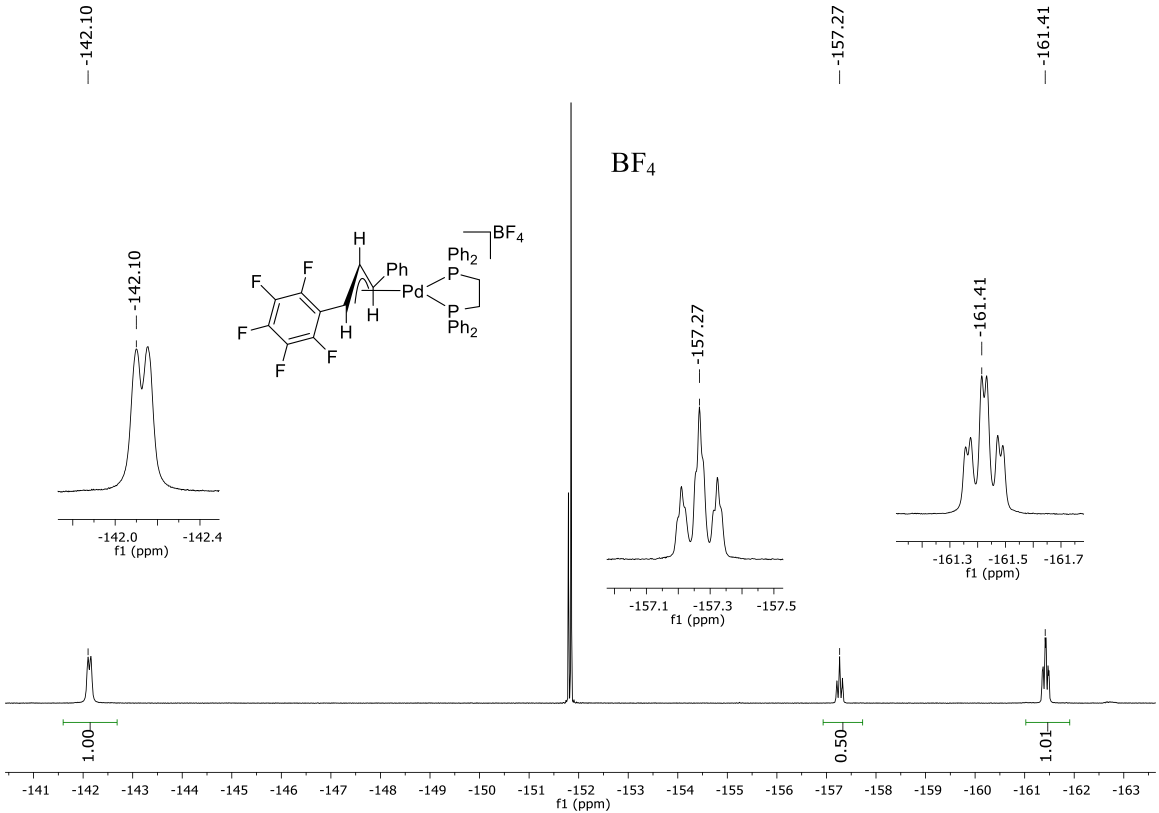

Figure S15. ^{19}F NMR (376.19 MHz, CDCl$_3$) of [Pd(dppe)(η^3-Ph-CH-CH-CH-Pf)](BF$_4$) (**4a**) at 298 K.

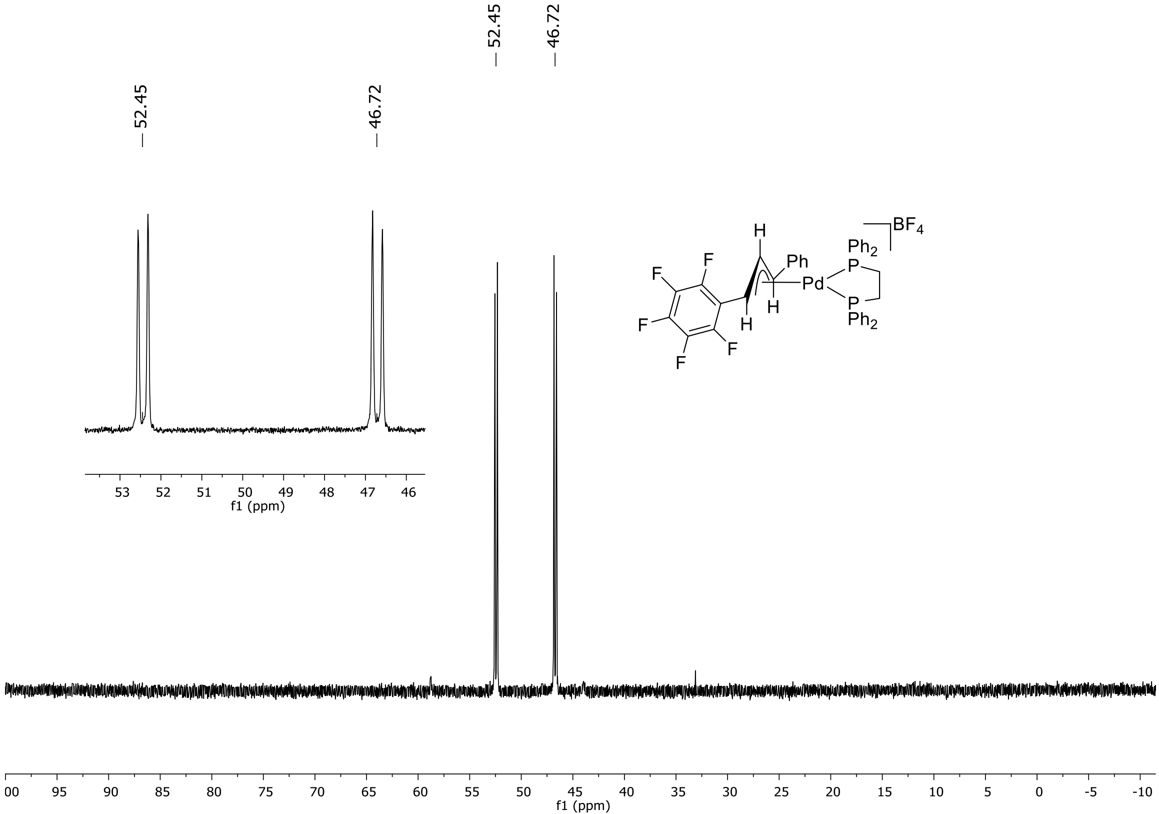

Figure S16. ^{31}P NMR (161.87 MHz, CDCl$_3$) of [Pd(dppe)(η^3-Ph-CH-CH-CH-Pf)](BF$_4$) (**4a**) at 298 K.

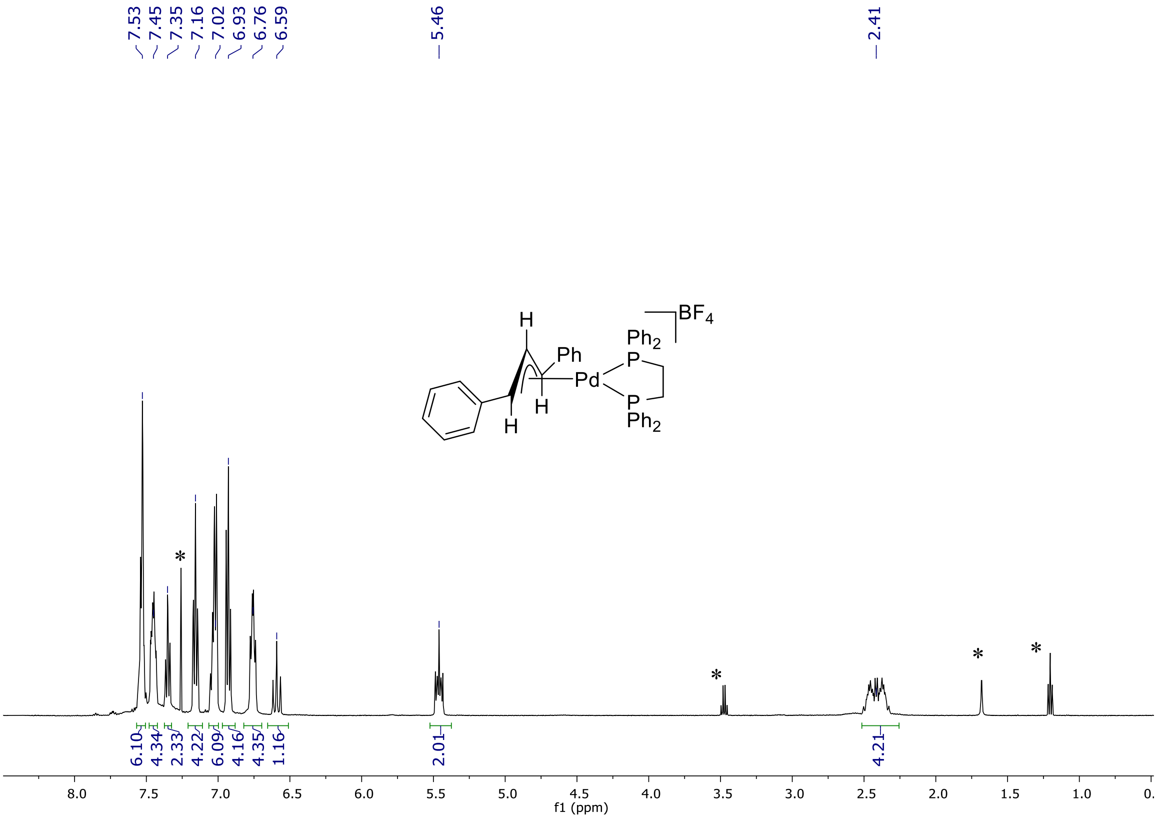

Figure S17. ^{1}H NMR (399.86 MHz, CDCl$_3$) of [Pd(dppe)(η^3-Ph-CH-CH-CH-Ph)](BF$_4$) (**4b**) at 298 K. * Signals corresponding to the solvent (H$_2$O, chloroform and diethylether).

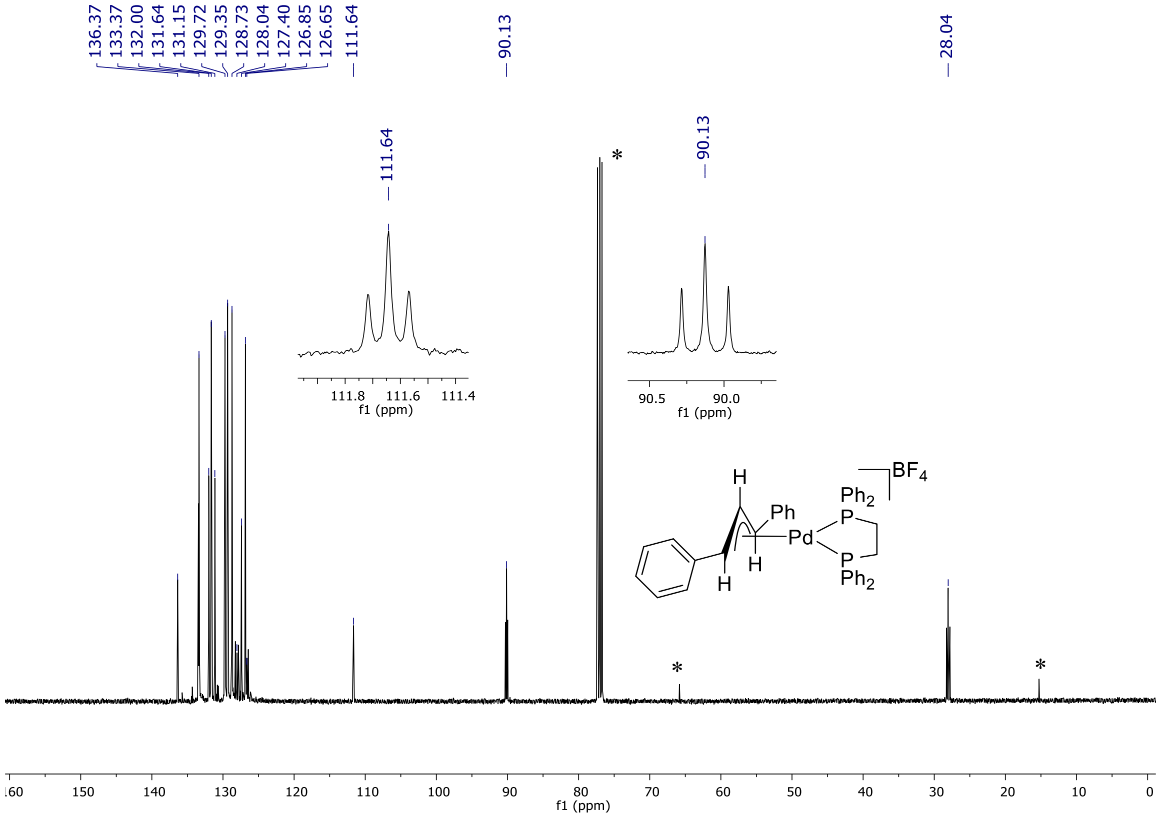

Figure S18. ^{13}C{^{1}H} NMR (100.56 MHz, CDCl$_3$) of [Pd(dppe)(η^3-Ph-CH-CH-CH-Ph)](BF$_4$) (**4b**) at 298 K. * Signals corresponding to the solvent (chloroform and diethylether).

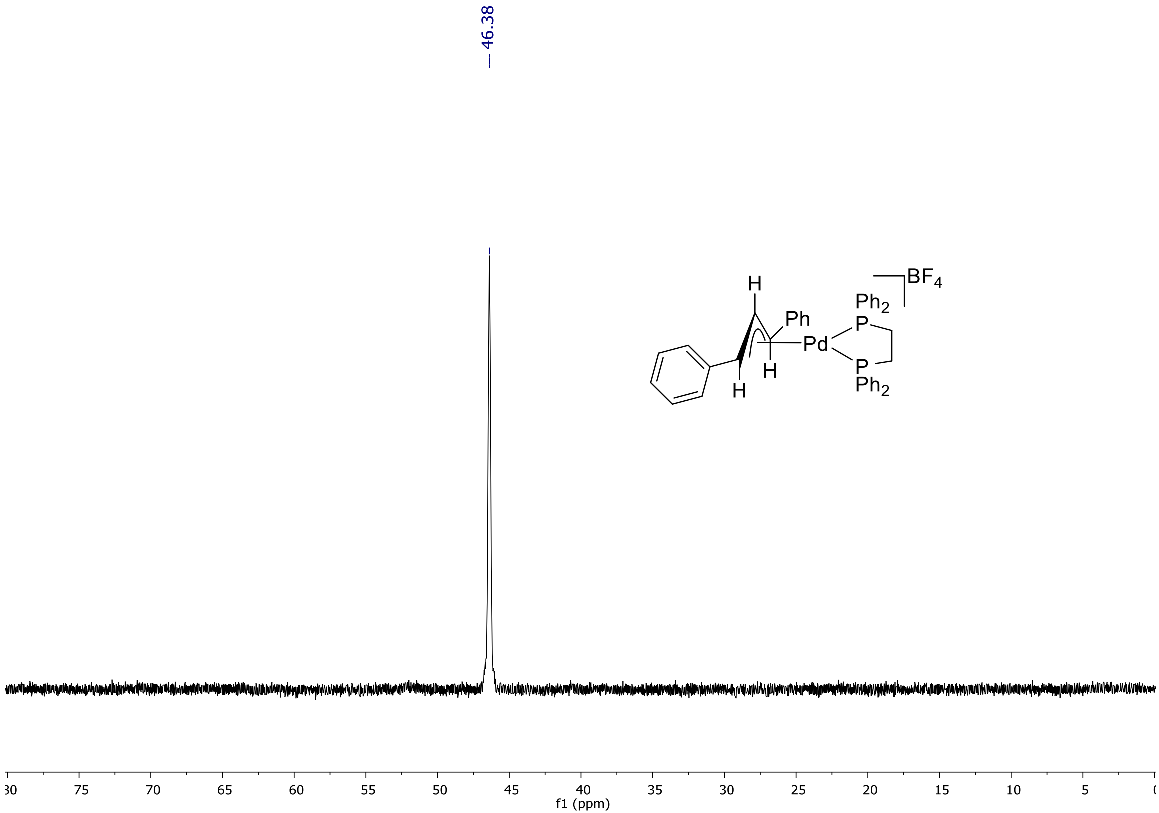

Figure S19. ^{31}P NMR (161.87 MHz, $CDCl_3$) of [Pd(dppe)(η^3-Ph-CH-CH-CH-Ph)](BF_4) (**4b**) at 298 K.

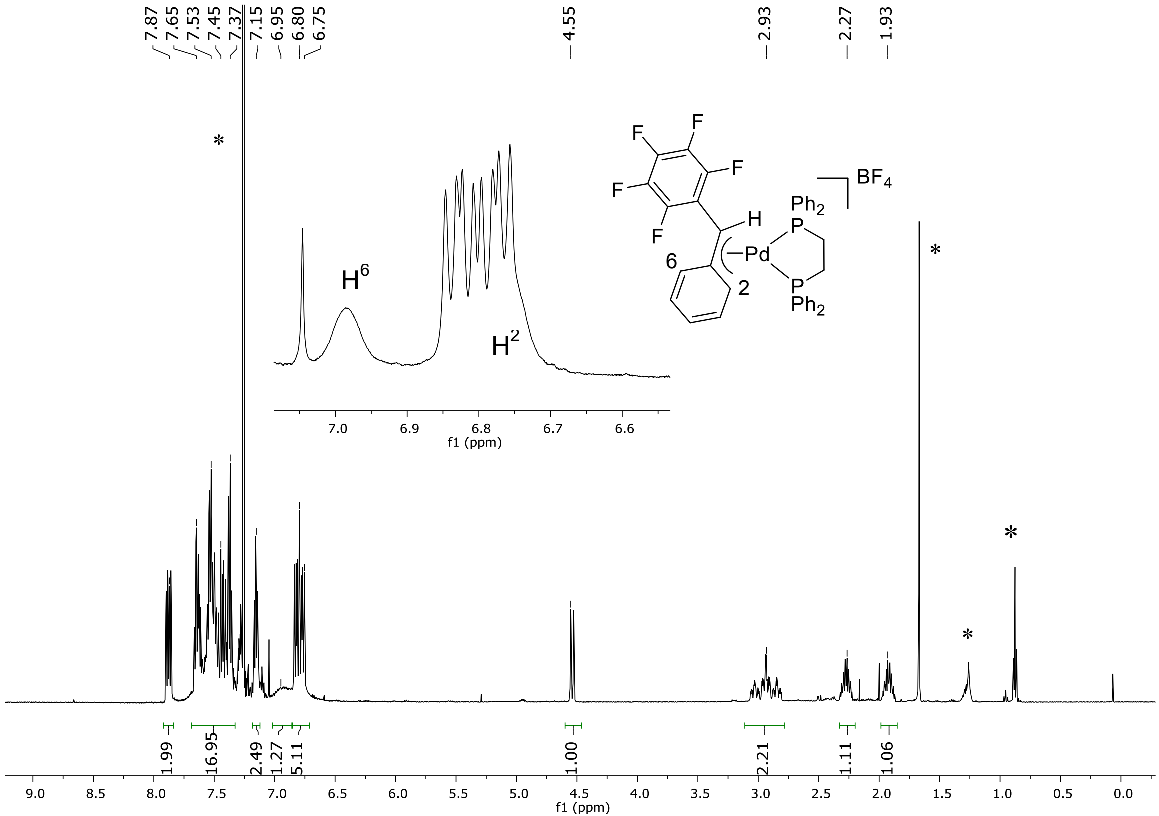

Figure S20. ^1H NMR (399.86 MHz, $CDCl_3$) of [Pd(dppe)(η^3-Ph-CH-CH-CH-Ph)](BF_4) (**6**) at 298 K. * Signals corresponding to the solvent (H_2O, chloroform and traces of hexanes). H^2 is overlapped with other signals at 6.8 ppm

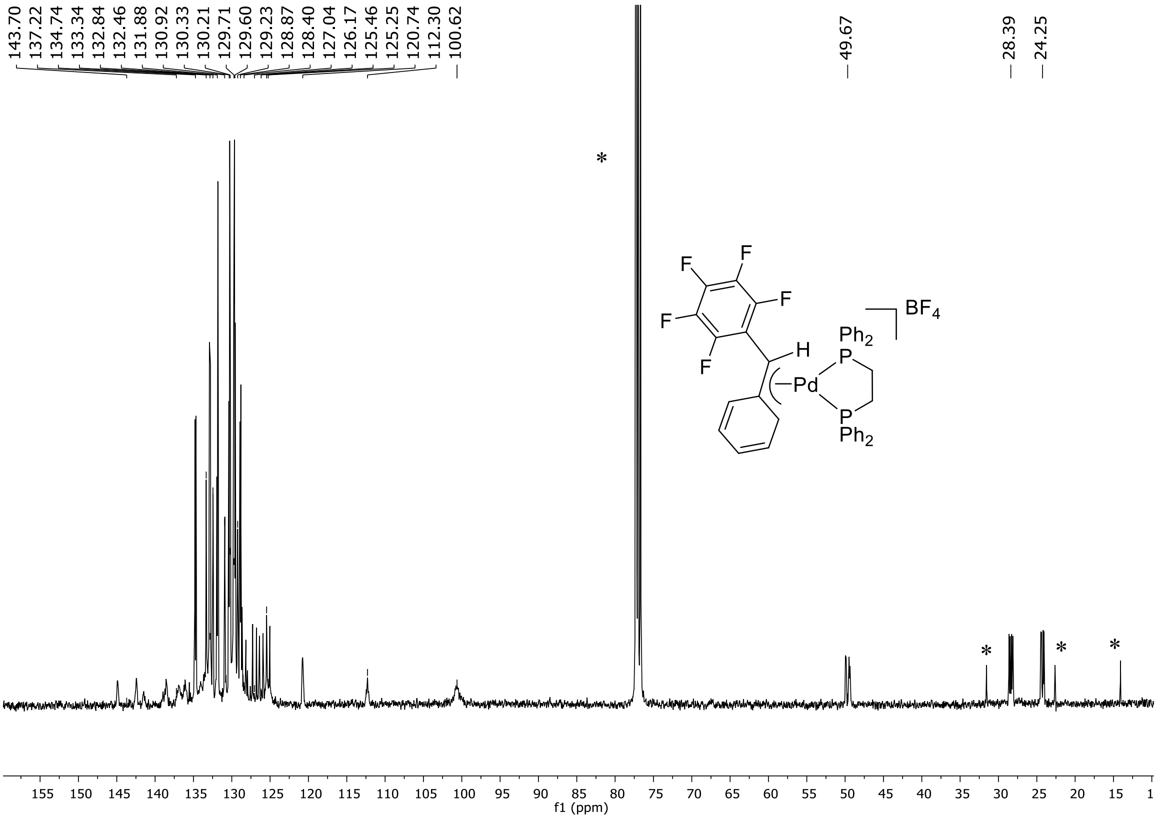

Figure S21. $^{13}C\{^{1}H\}$ NMR (100.56 MHz, $CDCl_3$) of [Pd(dppe)(η^3-Ph-CH-Pf)](BF_4) (**6**) at 298 K. * Signals corresponding to the solvent (chloroform and traces of hexanes).

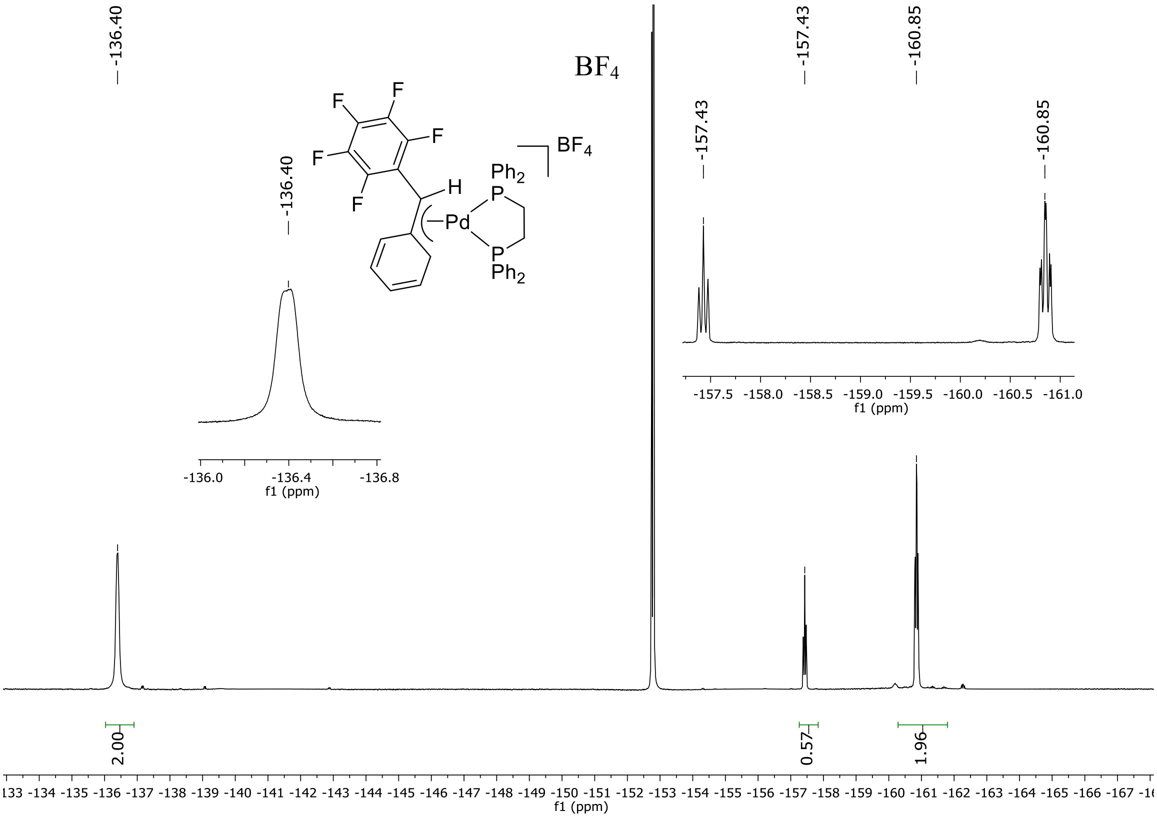

Figure S22. ^{19}F NMR (376.19 MHz, $CDCl_3$) of [Pd(dppe)(η^3-Ph-CH-Pf)](BF_4) (**6**) at 298 K.

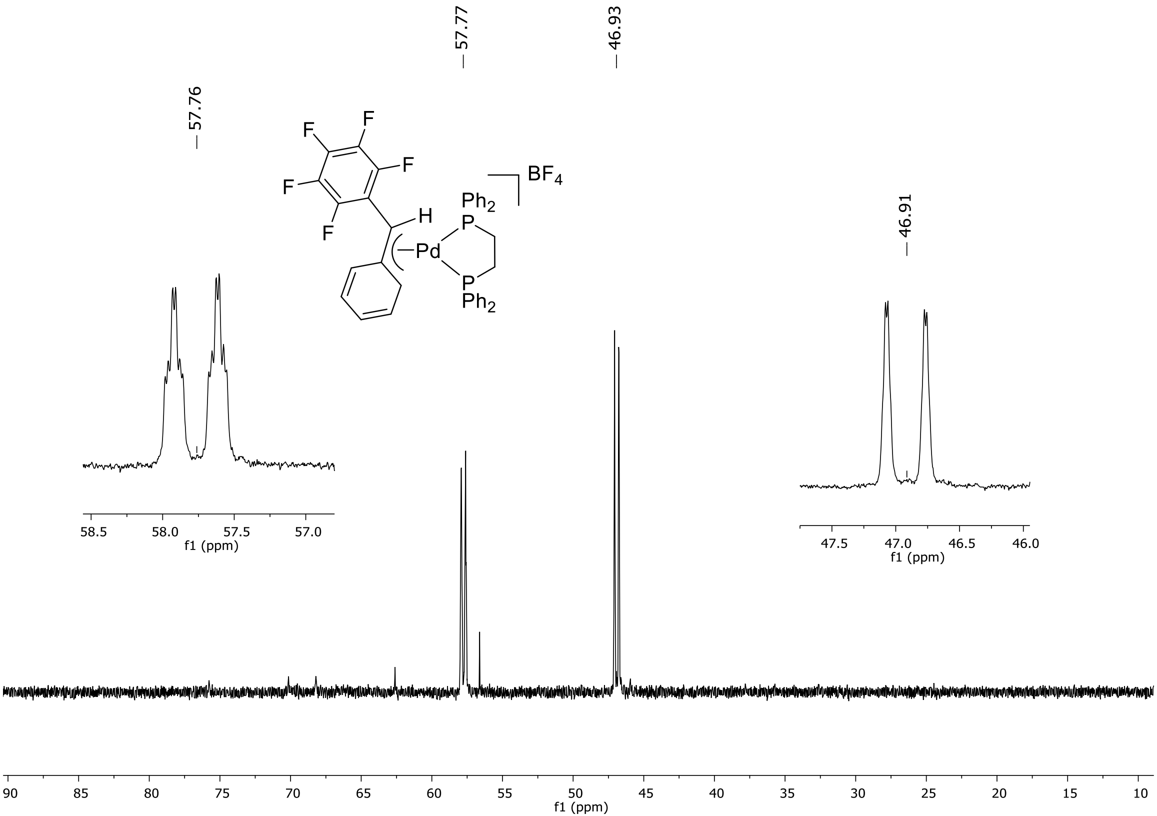

Figure S23. ^{31}P NMR (161.87 MHz, CDCl$_3$) of [Pd(dppe)(η^3-Ph-CH-Pf)](BF$_4$) (**6**) at 298 K.

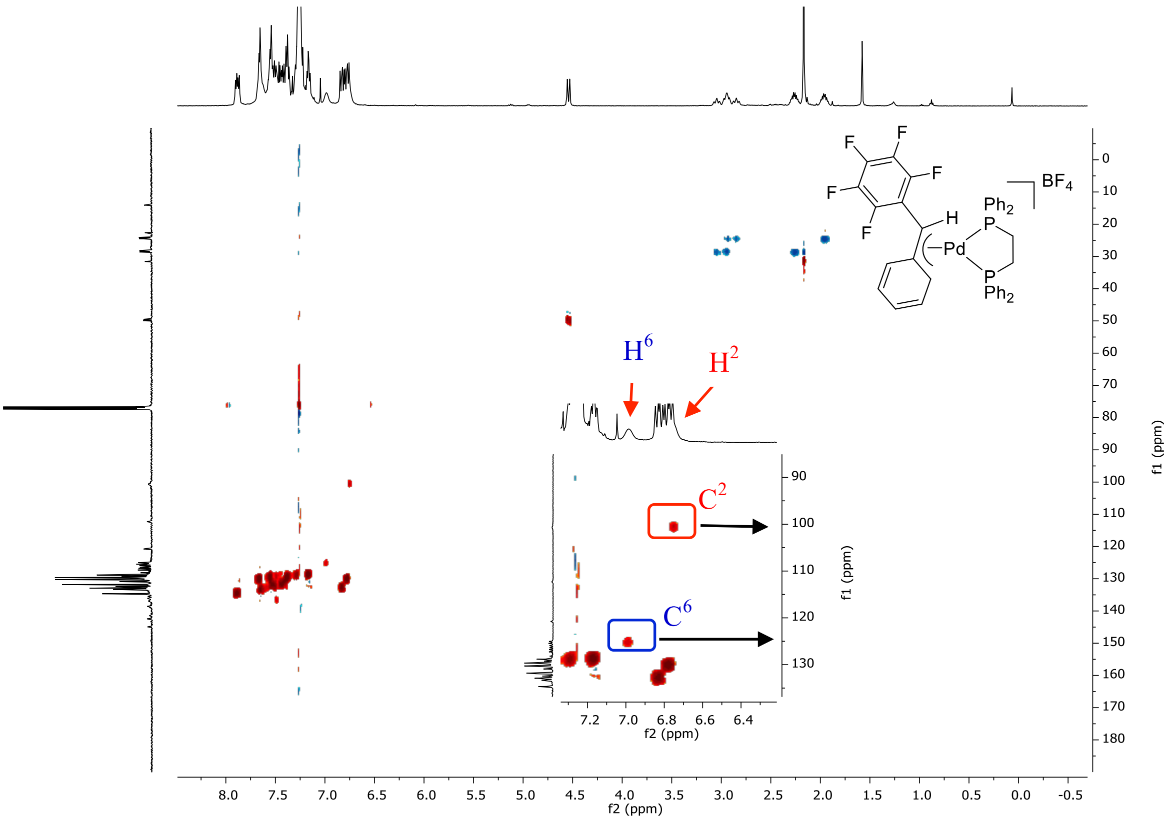

Figure S24. ^{1}H-^{13}C gHSQCAD NMR of [Pd(dppe)(η^3-Ph-CH-Pf)](BF$_4$) **(6)** in CDCl$_3$ at 298 K.

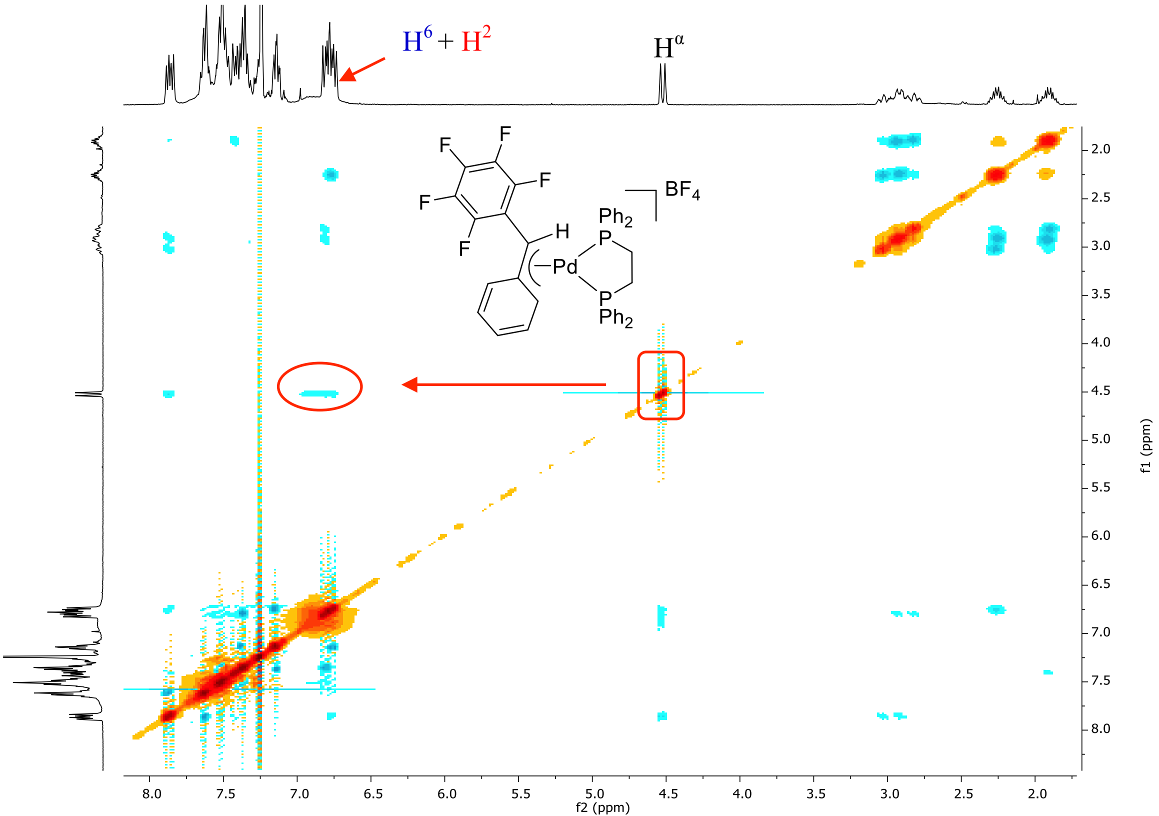

Figure S25. Phase sensitive ^1H 2D-ROESY NMR of [Pd(dppe)(η^3-Ph-CH-Pf)](BF_4) **(6)** in $CDCl_3$ at 298 K.

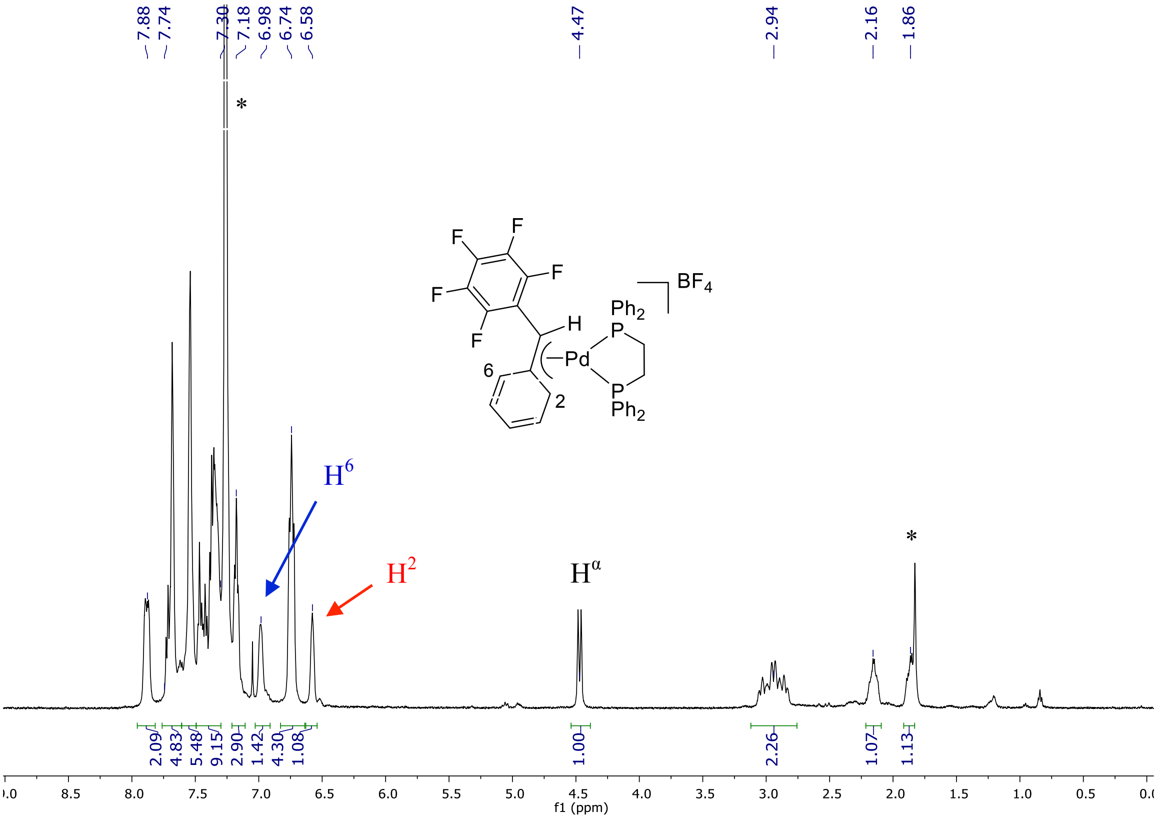

Figure S26. ^1H NMR (499.73 MHz, $CDCl_3$) of [Pd(dppe)(η^3-Ph-CH-CH-CH-Ph)](BF_4) (**6**) at 226 K. * Signals corresponding to solvents (H_2O and chloroform).

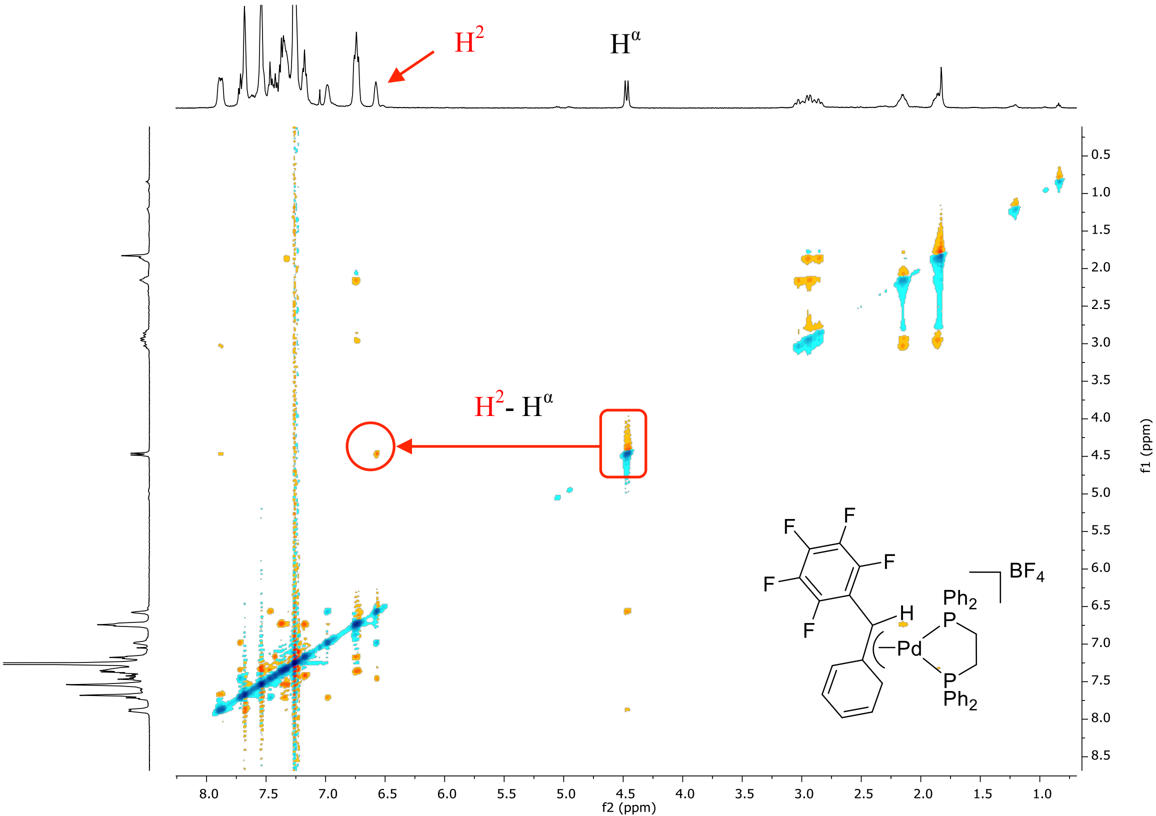

Figure S27. Phase sensitive ^{1}H 2D-ROESY NMR of [Pd(dppe)(η^3-Ph-CH-Pf)](BF$_4$) **(6)** in CDCl$_3$ at 226 K.

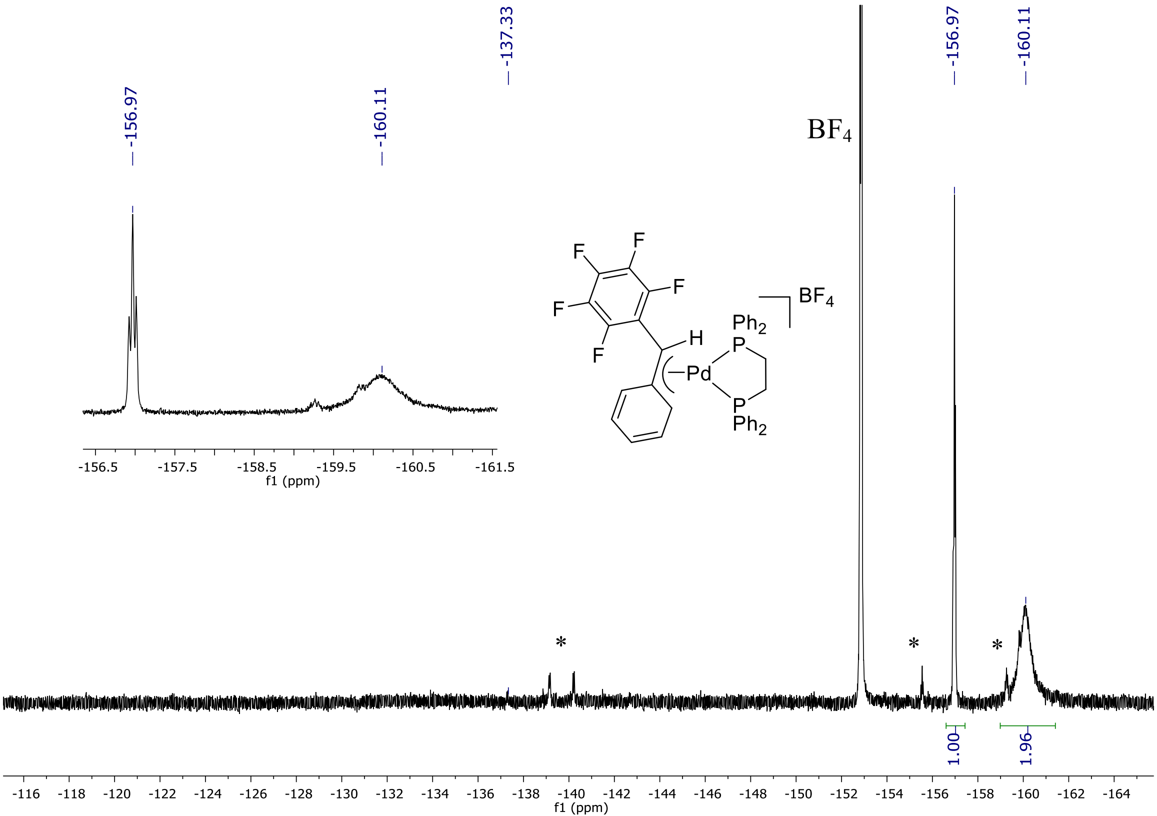

Figure S28. ^{19}F NMR (470.17 MHz, CDCl$_3$) of [Pd(dppe)(η^3-Ph-CH-Pf)](BF$_4$) (**6**) at 226 K. The F$_{ortho}$ signals are not visible due to coalescence at this temperature * Decomposition species from **6**.

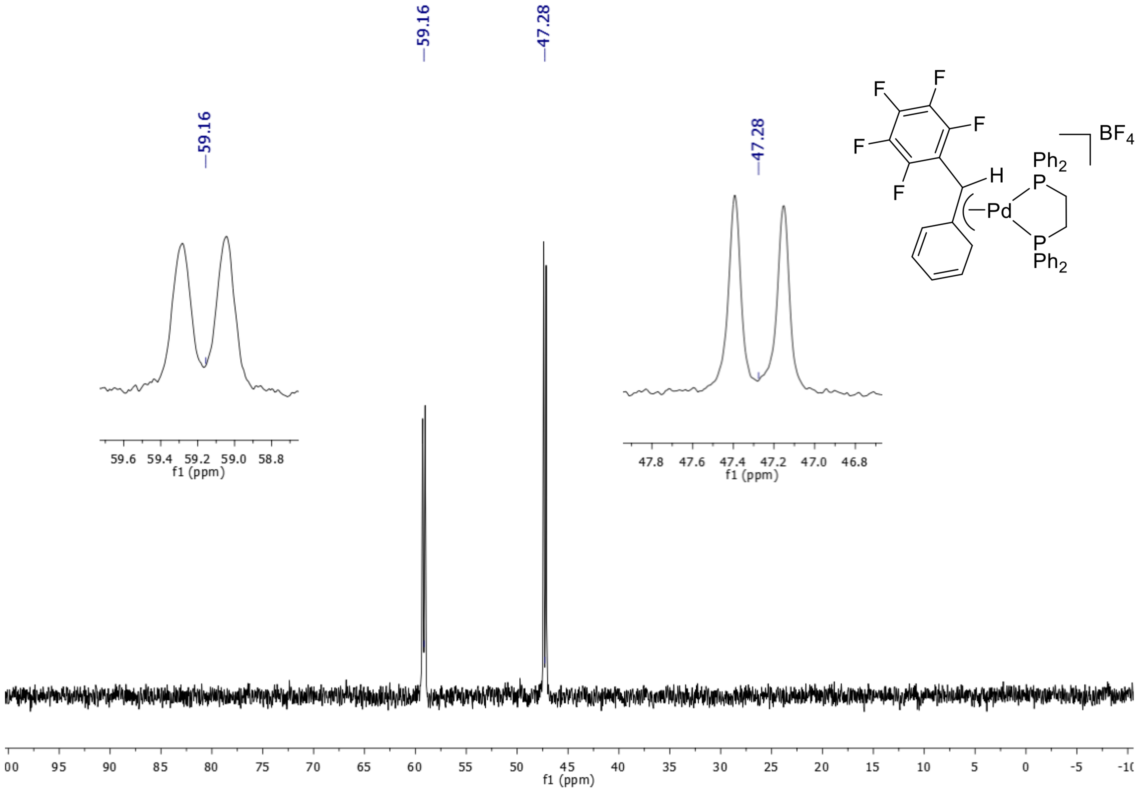

Figure S29. ^{31}P NMR (202.31 MHz, CDCl$_3$) of [Pd(dppe)(η^3-Ph-CH-Pf)](BF$_4$) (**6**) at 226 K.

5. References

1 C. Ammann, P. Meier and A. Merbach, *J. Magn. Reson.* 1982, **46**, 319–321.

2 (a) H. Morrison, S. Danishefsky and P. Yates, *J. Org. Chem.* 1961, **26**, 2617–2618; (b) M. P. Doyle and M. Yan, *J. Org. Chem.* 2002, **67**, 602–604; (c) F. Friscourt, C. J. Fahrni and G. -J. Boons, *Chem. Eur. J.* 2015, **21**, 13996–14001.

3 R. Usón, J. Forniés, J. A. Nalda, M. J. Lozano, P. Espinet and A. C. Albéniz, *Inorg. Chim. Acta* 1989, **156**, 251–256.

4 M. A. Zhuravel, D. S. Glueck, C. D. Incarvito and A. L. Rheingold, *Organometallics* 1999, **18**, 4673–4676.

5 (a) C. S. Shultz, J. Ledford, J. M. DeSimone and M. Brookhart, *J. Am. Chem. Soc.* 2000, **122**, 6351–6356; (b) J. Ledford, C. S. Shultz, D. P. Gates, P. S. White, J. M. DeSimone and M. Brookhart, *Organometallics* 2001, **20**, 5266–5276.

6 CrysAlisPro Software system, version 1.171.33.51, 2009, Oxford Diffraction Ltd, Oxford, UK.

7 G. M. Sheldrick, *Acta Cryst.*, 2015, **C71**, 3-8.

8 O. V Dolomanov, L. J. Bourhis, R. J. Gildea, J. A. K. Howard and H. Puschmann, *J. Appl. Crystallogr.* 2009, **42**, 339–34.

9 Y. Zhao and D. G. Truhlar, *J. Chem. Phys.* 2006, **125**, 194101.

10 Y. Zhao and D. G. Truhlar, *Theor. Chem. Acc.* 2008, **120**, 215–241.

11 Gaussian 09, Revision D.01, M. J. Frisch, G. W. Trucks, H. B. Schlegel, G. E. Scuseria, M. A. Robb, J. R. Cheeseman, G. Scalmani, V. Barone, G. A. Petersson, H. Nakatsuji, X. Li, M. Caricato, A. Marenich, J. Bloino, B. G. Janesko, R. Gomperts, B. Mennucci, H. P. Hratchian, J. V. Ortiz, A. F. Izmaylov, J. L. Sonnenberg, D. Williams-Young, F. Ding, F. Lipparini, F. Egidi, J. Goings, B. Peng, A. Petrone, T. Henderson, D. Ranasinghe, V. G. Zakrzewski, J. Gao, N. Rega, G. Zheng, W. Liang, M. Hada, M. Ehara, K. Toyota, R. Fukuda, J. Hasegawa, M. Ishida, T. Nakajima, Y. Honda, O. Kitao, H. Nakai, T. Vreven, K. Throssell, J. A. Montgomery, Jr., J. E. Peralta, F. Ogliaro, M. Bearpark, J. J. Heyd, E. Brothers, K. N. Kudin, V. N. Staroverov, T. Keith, R. Kobayashi, J. Normand, K. Raghavachari, A. Rendell, J. C. Burant, S. S. Iyengar, J. Tomasi, M. Cossi, J. M. Millam, M. Klene, C. Adamo, R. Cammi, J. W. Ochterski, R. L. Martin, K. Morokuma, O. Farkas, J. B. Foresman, and D. J. Fox, Gaussian, Inc., Wallingford CT, 2009.

12 M. M. Francl, W. J. Pietro, W. J. Hehre, J. S. Binkley, M. S. Gordon, D. J. DeFrees and J. A. Pople, *J. Chem. Phys.* 1982, **77**, 3654–3665.

13 T. Clark, J. Chandrasekhar, G. W. Spitznagel and P. V. R. Schleyer, *J. Comput. Chem.* 1983, **4**, 294–301.

14 A. W. Ehlers, M. Böhme, S. Dapprich, A. Gobbi, A. Höllwarth, V. Jonas, K. F. Köhler, R. Stegmann, A. Veldkamp and G. Frenking, *Chem. Phys. Lett.* 1993, **208**, 111–114.

15 L. E. Roy, P. J. Hay and R. L. Martin, *J. Chem. Theory Comput.* 2008, **4**, 1029–1031.